

Dear authors,

Thank you for your revision and clarifications. However, there are still spelling mistakes and grammatical problems with your most recent changes to the manuscript (listed below). This is somewhat frustrating as these could have easily been avoided. I therefore have to ask for yet another revision. This should really be the last so please ensure that your next manuscript is of the best possible quality.

All the best,

Dear Charles Mullan,

We are very pleased to re-submit our manuscript to PCI evolutionary biology. We corrected all the problems that you listed. Moreover we did a proofreading of our manuscript, putting lot of attention on the most recent changes.

Sincerely yours,

Ludovic Maisonneuve, on behalf of all authors.

Evolution and genetic architecture of disassortative mating at a locus under heterozygote advantage

Ludovic Maisonneuve^{1,*}, Mathieu Chouteau², Mathieu Joron³ and Violaine Llaurens¹

1. Institut de Systematique, Evolution, Biodiversité (UMR7205), Museum National d'Histoire Naturelle, CNRS, Sorbonne-Université, EPHE, Université des Antilles, CP50, 57 rue Cuvier, 75005 Paris, France;

2. Laboratoire Ecologie, Evolution, Interactions Des Systèmes Amazoniens (LEEISA), USR 3456, Université De Guyane, IFREMER, CNRS Guyane, 275 route de Montabo, 97334 Cayenne, French Guiana;

3. (CEFE), Univ Montpellier, CNRS, EPHE, IRD, Univ Paul Valéry Montpellier 3, Montpellier, France;

* Corresponding author: Ludovic Maisonneuve; e-mail: ludovic.maisonneuve.2015@polytechnique.org.

Manuscript elements: Table 1, Table 2, figure 1, figure 2, figure 3, figure 4, figure 5, figure S5, figure S5, figure S7, figure S8, figure S9, figure S10, figure S11.

Keywords: Disassortative mating, Supergene, Frequency dependent selection, genetic load, mate preference, *Heliconius numata*.

Manuscript type: Article.

Abstract

2 The evolution of mate preferences may depend on natural selection acting on the mating cues
and on the underlying genetic architecture. While the evolution of assortative mating with re-
4 spect to locally adapted traits has been well-characterized, the evolution of disassortative mating
is poorly characterized. Here we aim at understanding the evolution of disassortative mating for
6 traits under strong balancing selection, by focusing on polymorphic mimicry as an illustrative
example. Positive frequency-dependent selection exerted by predators generates local selection
8 on wing patterns acting against rare variants and promoting local monomorphism. This acts
across species boundaries, favouring Mullerian mimicry among defended species. In this well-
10 characterized adaptive landscape, polymorphic mimicry is rare but is observed in a butterfly
species, associated with polymorphic chromosomal inversions. Because inversions are often as-
12 sociated with recessive deleterious mutations, we hypothesize they may induce heterozygote
advantage at the color pattern locus, putatively favoring the evolution of disassortative mating.
14 To explore the conditions underlying the emergence of disassortative mating, we modeled both
a trait locus (colour pattern for instance), subject to mutational load, and a preference locus. We
16 confirm that heterozygote advantage favors the evolution of disassortative mating and show that
disassortative mating is more likely to emerge if at least one allele at the trait locus is free from
18 any recessive deleterious mutations. We modelled different possible genetic architectures under-
lying mate choice behaviour, such as self referencing alleles, or specific preference or rejection
20 alleles. Our results showed that self referencing or rejection alleles linked to the color pattern lo-
cus can be under positive selection and enable the emergence of disassortative mating. However
22 rejection alleles allow the emergence of disassortative mating only when the color pattern and
preference loci are tightly linked. Our results therefore provide relevant predictions on both the
24 selection regimes and the genetic architecture favoring the emergence of disassortative mating
and a theoretical framework in which to interpret empirical data on mate preferences in wild
26 populations.

Introduction

28 Mate preferences often play an important role in shaping trait diversity in natural populations,
but the mechanisms responsible for their emergence often remain to be characterized. While the
30 evolution of assortative mating on locally adapted traits is relatively well understood (Otto et al.,
2008; de Cara et al., 2008; Thibert-Plante and Gavrilets, 2013), the selective forces involved in
32 the evolution of disassortative mating are still largely unknown. Disassortative mating, *i.e.* the
preferential mating between individuals displaying different phenotypes, is a rare form of mate
34 preference (Jiang et al., 2013). In populations where individuals tend to mate with phenotypically
distinct partners, individuals with a rare phenotype have a larger number of available mates, re-
36 sulting in a higher reproductive success. By generating negative frequency-dependent selection
on mating cues, disassortative mating is often regarded as a process generating and/or maintain-
38 ing polymorphism within populations. Obligate disassortative mating leads to the persistence
of intermediate frequencies of sexes or mating types (Wright, 1939), and promotes polymor-
40 phism (e.g. the extreme case of some Basidiomycete fungi where thousands of mating types are
maintained (Casseltan, 2002)). Disassortative mating can be based on different traits. Disassor-
42 tative mating based on odors is known to operate in mice (Penn and Potts, 1999) and humans
(Wedekind et al., 1995). Odor profiles are associated with genotype at the MHC loci affecting
44 the immune response, known to be under strong balancing selection (Piertney and Oliver, 2006).
Balancing selection on MHC alleles partly stems from heterozygous advantage, whereby het-
46 erozygous genotypes might confer an ability to recognize a larger range of pathogens. Such het-
erozygote advantage may promote the evolution of disassortative mating (Tregenza and Wedell,
48 2000). Extreme examples of heterozygote advantage are observed for loci with reduced homozy-
gote survival. In the seaweed fly *Coelopa frigida* heterozygotes ($\alpha\beta$) at the locus *Adh* have a higher
50 fitness than homozygotes ($\alpha\alpha$ or $\beta\beta$) (Butlin et al., 1984; Mérot et al., 2019) and females prefer
males with a genotype that differs from their own (Day and Butlin, 1987). In the white-throated
52 sparrow *Zonotrichia albicollis*, strong disassortative mating is known to operate with respect to

the color of the head stripe and associated with chromosomal dimorphism (Throneycroft, 1975).
54 This plumage dimorphism is associated with a spectacular chromosomal polymorphism (Tuttle
et al., 2016), with a complete lack of homozygous individuals for the rearranged chromosome
56 (Horton et al., 2013).

While the fitness advantage of disassortative mating targeting loci with overdominance seems
58 straightforward, the genetic basis of disassortative preferences remains largely unknown. One
exception is the self-incompatibility system in *Brassicaceae* where the S-locus determines a spe-
60 cific rejection of incompatible pollens (Hiscock and McInnis, 2003). S-haplotypes contain tightly
linked, co-evolved SCR and SRK alleles, encoding for a protein of the pollen coat and a receptor
62 kinase located in the pistil membrane respectively, preventing fertilization from self-incompatible
pollen due to specific receptor-ligand interactions. Self-rejection has also been proposed as an ex-
64 planation for the disassortative mating associated with odor in humans. Body odors are strongly
influenced by genotypes at the immune genes HLA and rejection of potential partners has been
66 shown to be related to the level of HLA similarity, rather than to a particular HLA genotype
(Wedekind and Furi, 1997). In the white-throated sparrow, disassortative mating results from
68 specific preferences for color plumage that differ between males and females; *tan*-striped males
are preferred by all females while *white*-striped females are preferred by all males (Houtman and
70 Falls, 1994). Different mechanisms leading to mate preferences and associated genetic archite-
cture can be hypothesized, that may involve the phenotype of the chooser. Based on the categories
72 described by Kopp et al. (2018), we assume that disassortative mating can emerge from two main
mechanisms. (1) *Self-referencing*, when an individual uses its own signal to choose its mate, which
74 may generate a disassortative mating that depends on the phenotypes of both the choosing and
the chosen partners. (2) Preferences for or rejection of a given phenotype in the available part-
76 ners (*recognition/trait* hypothesis), independently from the phenotype of the choosing partner,
may also enable the emergence of disassortative mate preferences. These two mechanisms could
78 involve a two locus architecture where one locus controls the mating cue and the other one the
preference towards the different cues (Kopp et al., 2018). The level of linkage disequilibrium

80 between the two loci could have a strong impact on the evolution of disassortative mating. In
models investigating the evolution of assortative mating on locally-adapted traits, theoretical
82 simulations have demonstrated that assortative mating is favored when the preference and the
cue loci are linked (Kopp et al., 2018).

84 Here we explore the evolutionary forces leading to the emergence of disassortative mating.
We use as a model system the specific case of the butterfly species *Heliconius numata*, where
86 high polymorphism in wing pattern is maintained within populations (Joron et al., 1999) and
strong disassortative mating operates between wing pattern forms (Chouteau et al., 2017). *H.*
88 *numata* butterflies are chemically-defended (Arias et al., 2016; Chouteau et al., 2019), and their
wing patterns act as warning signals against predators (Chouteau et al., 2016a). At a local scale,
90 natural selection on local mimicry usually leads to the fixation of a single warning signal shared
by multiple defended species (Müllerian mimicry) (Mallet and Barton, 1989). However, local
92 polymorphism of mimetic color patterns is maintained in certain species for instance under a
balance between migration and local selection on mimicry (Joron and Iwasa, 2005). Yet, the level
94 of polymorphism observed within populations of *H. numata* (Joron et al., 1999) would require
that the strong local selection is balanced by a very high migration rate. However, disassortative
96 mating based on wing pattern operates in *H. numata*, with females rejecting males displaying
the same color pattern (Chouteau et al., 2017). Such disassortative mating could enhance local
98 polymorphism in color pattern within this species. Nevertheless, the mode of evolution of a
disassortative mating is unclear, notably because preferences for dissimilar mates should not
100 be favoured if natural selection by predators on adult wing pattern acts against rare morphs
(Chouteau et al., 2016b). Building on this well-documented case study, we use a theoretical
102 approach to provide general predictions on the evolution of disassortative mating in polymorphic
traits, and on expected genetic architecture underlying this behavior.

104 Variation in wing color pattern in *H. numata* is controlled by a single genomic region, called
the supergene P (Joron et al., 2006), displaying distinct chromosomal inversion combinations,
106 each associated with a distinct mimetic phenotype (Joron et al., 2011). These inversions have

recently been shown to be associated with a significant genetic load, resulting in a strong heterozygote advantage (Jay et al., 2019). We thus investigate whether a genetic load associated with locally adaptive alleles may favor the evolution of mate preference and promote local polymorphism. We then explore two putative genetic architectures for mate preferences based on (1) *self referencing* and (2) based on a *recognition/trait* rule, and test for their respective impacts on the evolution of disassortative mating. Under both hypotheses, we assumed that the mating cue and the mating preference were controlled by two distinct loci, and investigate the effect of linkage between loci on the evolution of disassortative mating.

Methods

Model overview

Based on earlier models of Müllerian mimicry (Joron and Iwasa, 2005; Llaurens et al., 2013), we describe the evolution of mate preferences based on color pattern using ordinary differential equations (ODE). We track the density of individuals carrying different genotypes combining the alleles at the locus P controlling mimetic color pattern and at the locus M underlying sexual preference. We assume a diploid species, so that each genotype contains four alleles.

The set of all possible four-allele genotypes is defined as $\mathcal{G} = \mathcal{A}_P \times \mathcal{A}_P \times \mathcal{A}_M \times \mathcal{A}_M$ where $\mathcal{A}_P, \mathcal{A}_M$ are the set of alleles at locus P and M respectively. A given genotype is then an quadruplet of the form (p_m, p_f, m_m, m_f) with $p_m \in \mathcal{A}_P$ and $m_m \in \mathcal{A}_M$ (resp. p_f and m_f) being the alleles at loci P and M on the maternal (resp. paternal) chromosomes. A recombination rate ρ between the color pattern locus P and the preference locus M is assumed.

We consider two geographic patches numbered 1 and 2 where those genotypes can occur. For all $(i, n) \in \mathcal{G} \times \{1, 2\}$ we track down the density of individuals of each genotype i within each patch n , $N_{i,n}$ through time. Following previous models, polymorphism in mimetic color pattern is maintained within each of the two patches, by a balance between (1) local selection on color pattern in opposite directions in the two patches and (2) migration between patches.

132 The evolution of genotype densities through time, for each patch, is influenced by predation,
 mortality, migration between patches and reproduction, following the general equations :

$$\forall (i, n) \in \mathcal{G} \times \{1, 2\} \quad \frac{d}{dt} N_{i,n} = Pred_{i,n} + Mort_{i,n} + Mig_{i,n} + Rep_{i,n}, \quad (1)$$

134 where $Pred_{i,n}$, $Rep_{i,n}$, $Mig_{i,n}$, and $Mort_{i,n}$ described the respective contributions of these four
 processes to the change in density of genotype i within each patch n . The computation of each
 136 of these four contributions is detailed in specific sections below. All variables and parameters are
 summarized in Table 1 and 2 respectively.

138 Since our ODE model describes the change in genotype densities at a population level, this
 amounts to considering that predation, migration, reproduction and survival occur simultane-
 140 ously (see Equation (1)). In a large population, we can assume that predation, migration, re-
 production and survival indeed occur in different individuals at the same time. Such a model
 142 implies that generations are overlapping and that there is no explicit ontogenic development:
 each newborn individual instantaneously behaves as an adult individual and can immediately
 144 migrate and reproduce. Our deterministic model provides general predictions while ignoring
 the effects of stochastic processes such as genetic drift.

146 *Mimetic color pattern alleles at locus P*

At the color pattern locus P , three alleles are assumed to segregate, namely alleles a , b and c ,
 148 encoding for phenotypes A , B and C respectively. The set of alleles at locus P is then $\mathcal{A}_P =$
 $\{a, b, c\}$. We assume strict dominance among the three alleles with $a > b > c$ in agreement with
 150 the strict dominance observed among supergene P alleles within natural populations of *H. numata*
 (Le Poul et al., 2014) and in other supergenes (Wang et al., 2013; Tuttle et al., 2016; Küpper et al.,
 152 2016). The three color pattern phenotypes are assumed to be perceived as categorically different
 by both mating partners and predators. We note CP the function translating each genotype i
 154 into the corresponding color pattern phenotype \mathcal{G} . For example, for all $(m_m, m_f) \in \mathcal{A}_M \times \mathcal{A}_M$,
 $CP((a, b, m_m, m_f)) = A$ because allele a is dominant over b and the color pattern phenotype

156 depends only on alleles at locus P . Each color pattern allele is also assumed to carry an individual
genetic load expressed when homozygous.

158 *Preference alleles at locus P*

We investigate the evolution of mate preference associated with color patterns, exploring in par-
160 ticular the conditions enabling the evolution of disassortative mating. We assume a single choosy
sex: only females can express preferences toward male phenotypes, while males have no pref-
162 erence and can mate with any accepting females. Female preferences toward males displaying
different color patterns are controlled by the locus M . We assume two different models of genetic
164 architecture underlying mate preferences: alleles at locus M determine either (1) a preference
toward similar or dissimilar phenotypes, which therefore also depends on the phenotype of the
166 choosing individual, following the *self-referencing* hypothesis or (2) a preference toward a given
color pattern displayed by the mating partner, independent of the color pattern of the choosing
168 individual, following the *recognition/trait* hypothesis.

Predation

170 The probability of predation on individuals depends on their mimetic color patterns controlled
by the locus P . Predation is determined in our model by a basic (patch-specific) effect of the
172 local community of prey favouring one of the wing patterns locally (local adaptation through
mimicry), itself modulated by positive frequency dependence of the different wing patterns con-
174 trolled by P , within the focal species population. This is detailed below.

Divergent local adaptation in color pattern

176 Local selection exerted by predators promotes convergent evolution of wing color patterns among
defended species (*i.e.* Müllerian mimicry, (Müller, 1879)), forming so-called mimicry rings com-
178 posed of individuals from different species displaying the same warning signal within a locality.

Mimicry toward the local community of defended prey therefore generates strong local selection
 180 on color pattern and the direction of this selection then varies across localities (Sherratt, 2006).

Here we assume two separate populations exchanging migrants of an unpalatable species
 182 involved in Müllerian mimicry with other chemically-defended species. Local communities of
 species involved in mimicry (*i.e.* mimicry rings) differ across localities. We consider two patches
 184 occupied by different mimetic communities: population 1 is located in a patch where the local
 community (*i.e.* other chemically-defended species, not including *H. numata*) mostly displays
 186 phenotype A, and population 2 in a patch where the mimetic community mostly displays pheno-
 type B. This spatial variation in mimicry rings therefore generates a divergent selection favouring
 188 distinct locally adapted phenotypes. Note that allele *c*, and corresponding phenotype C is non-
 mimetic in both patches and at a disadvantage in both patches. Every individual of the focal
 190 (polymorphic) species is exposed to a predation risk modulated by its resemblance to the local
 mimetic community of butterflies. Each genotype *i* in population *n* (with $(i, n) \in \mathcal{G} \times \{1, 2\}$)
 192 suffers from a basic predation mortality factor $d_{i,n}$. This parameter is lower for individuals dis-
 playing the phenotype mimetic to the local community (*i.e.* the phenotype A in population 1
 194 and B in population 2). Individuals displaying phenotype C being non-mimetic in both patches,
 suffer from a high predation risk in both patches.

Here, to simplify, we consider that this basic mortality factor takes the value d_m for the locally
 196 mimetic phenotype (A in patch 1, B in patch 2), and d_{n-m} for the locally non-mimetic phenotypes
 198 (B and C in patch 1, A and C in patch 2). We therefore introduce parameters d_{n-m} and d_m , with
 $d_{n-m} > d_m$, as follows: the basic predation mortality factors for individuals not displaying and
 200 displaying the same color pattern as the local community respectively. For $i \in \mathcal{G}$, the basic
 predation mortality factors of individuals with genotype *i* in patch 1 and 2 are

$$d_{i,1} = \mathbb{1}_{\{CP(i)=A\}}d_m + \mathbb{1}_{\{CP(i)\neq A\}}d_{n-m}, \quad (2)$$

$$d_{i,2} = \mathbb{1}_{\{CP(i)=B\}}d_m + \mathbb{1}_{\{CP(i)\neq B\}}d_{n-m}, \quad (3)$$

202 where $\mathbb{1}$ is the indicator function which return 1 if the condition under brace in true and 0
 else.

204 *Local positive frequency-dependent predation*

Predation exerted on a given phenotype depends on its match to the local mimetic environment
 206 (described by the parameter $d_{i,n}$ for all $(i, n) \in \mathcal{G} \times \{1, 2\}$, see previous paragraph), but also
 on its own abundance in the patch predators learn to associate warning patterns with chemi-
 208 cal defense. This learning behavior generates positive frequency-dependent selection on color
 patterns (Chouteau et al., 2016b): displaying a widely shared color pattern decreases the risk of
 210 encountering a naive predator (Sherratt, 2006). Number-dependent predator avoidance in the
 focal species is assumed to depend on its unpalatability coefficient (λ) and on the density of each
 212 phenotype within the population: the protection gained by phenotypic resemblance is greater for
 higher values of the unpalatability coefficient λ . For $(i, n) \in \mathcal{G} \times \{1, 2\}$, the change in the density
 214 of a genotype i in patch n due to predation thus takes into account both the spatial variation in
 mimetic communities (using $d_{i,n}$) modulated by the local frequency-dependent selection, and is
 216 thus described by the equation:

$$Pred_{i,n} = -\frac{d_{i,n}N_{i,n}}{1 + \lambda \sum_{j \in \mathcal{G}} \mathbb{1}_{\{CP(i)=CP(j)\}}N_{j,n}}, \quad (4)$$

218 where $\sum_{j \in \mathcal{G}} \mathbb{1}_{\{CP(i)=CP(j)\}}N_{j,n}$ is the total density, within patch n , of individuals sharing the
 same color pattern as individuals of genotype i .

Mortality

220 We assume a baseline mortality rate δ . The recessive genetic loads $\delta_a, \delta_b, \delta_c$ associated with the
 respective alleles a, b and c limit the survival probabilities of homozygous genotypes at locus P .

222 For $i = (p_m, p_f, m_m, m_f) \in \mathcal{G}, n \in \{1, 2\}$ the change in density of individuals with genotype i
 in patch n is given by

$$Mort_{i,n} = -(\delta + (\mathbb{1}_{\{p_m=p_f=a\}}\delta_a + \mathbb{1}_{\{p_m=p_f=b\}}\delta_b + \mathbb{1}_{\{p_m=p_f=c\}}\delta_c))N_{i,n}. \quad (5)$$

224

Migration

We assume a constant symmetrical migration rate mig corresponding to a proportion of individuals migrating from one patch to the other, as classically assumed in population genetics models (see for instance Holt (1985); Kuang and Takeuchi (1994); Joron and Iwasa (2005)). The number of individuals of each of the genotypes migrating to the other patch is therefore directly proportional to their density in their source population. For $(i, n, n') \in \mathcal{G} \times \{1, 2\} \times \{1, 2\}, n \neq n'$, the change in the density of individuals with genotype i in patch n due to migration between patches n and n' is given by the difference between the density of individuals coming into the patch $migN_{i,n'}$ and those leaving the patch $migN_{i,n}$:

$$Mig_{i,n} = migN_{i,n'} - migN_{i,n}. \quad (6)$$

where mig is the migration coefficient $mig \in [0, 1]$.

234

Reproduction

In the model, the reproduction term takes into account the basic demographic parameter, the effect of mate preference controlled by locus M and the fecundity limitations associated with choosiness.

Local demography

We assume that the populations from both patches have identical carrying capacity K and growth rate r . We name $N_{tot,n}$ the total density in patch n . The change in the total density due to reproduction is given by the logistic regulation function $r(1 - \frac{N_{tot,n}}{K})N_{tot,n}$. Thus for $(i, n) \in \mathcal{G} \times$

242 $\{1, 2\}$, the change in the density of genotype i in patch n generated by sexual reproduction is
 given by:

$$Rep_{i,n} = r(1 - \frac{N_{tot,n}}{K})N_{tot,n}F_{i,n}, \quad (7)$$

244 where $(F_{i,n})_{i \in \mathcal{G}}$ are the frequencies of each genotype in the progeny. These frequencies depend
 on the behavior of the female, controlled by the preference locus M and on the availability of the
 246 preferred partners in the population, as detailed in the following section.

Mate preferences

248 During sexual reproduction, we assume that only one out of the two sexes expresses a mate
 preference, as often observed in sexual reproduction where females are usually choosier. Thus
 250 we assume females to be the choosy sex. The mate preference of female is then considered strict,
 implying that choosy individuals never mate with individuals displaying their non-preferred
 252 phenotype. Two hypothetical mate preference mechanisms are investigated.

Under the *self-referencing* hypothesis (hyp 1), three alleles are assumed at loci M , coding for
 254 (i) random mating (r), (ii) assortative mating *sim* and (iii) disassortative *dis*) respectively (see fig.
 S5 for more details, $(\mathcal{A}_M = \{r, sim, dis\})$). We assume that the *self-referencing* preference alleles *sim*
 256 and *dis* are dominant to the random mating allele r (see fig. S5 for more details). The dominance
 relationship between the *sim* and *dis* alleles is not specified however, because we never introduce
 258 these two alleles together. Note that under the *self-referencing* hypothesis (hyp. 1), mate choice
 depends not only on the color pattern of the male, but also on the phenotype of the female
 260 expressing the preference.

The alternative mechanism of mate preference investigated, assumes a specific recognition
 262 of color patterns acting as mating cue (*recognition/trait*, hyp. 2). Under hyp. 2, four alleles
 segregate at locus M : allele m_r , coding for an absence of color pattern recognition (leading to
 264 random mating behavior), and m_a , m_b and m_c coding for specific recognition of color pattern
 phenotypes A , B and C ($\mathcal{A}_M = \{m_r, m_a, m_b, m_c\}$). The *no preference* allele m_r is recessive to all the

266 preference alleles m_a , m_b and m_c , and preference alleles are co-dominant, so that females with
heterozygous genotype at locus M may recognize two different color pattern phenotypes. Then,
268 the recognition enabled by preference alleles m_a , m_b and m_c triggers either *attraction* (hyp. 2.a) or
rejection (hyp. 2.b) toward the recognized color pattern, leading to assortative or disassortative
270 mating depending on the genotype i of the female and the color pattern phenotype of the male
(see figure S6 and S7 for more details).

272 *Genotype frequencies in the progeny*

We assume separate sexes and obligate sexual reproduction, and therefore compute explicitly the
274 Mendelian segregation of alleles during reproduction, assuming a recombination rate ρ between
the color pattern locus P and the preference locus M . We assume that the frequency of male
276 and female of a given phenotype is the same. For $(i, n) \in \mathcal{G} \times \{1, 2\}$, the frequency of genotype
 i in the progeny in patch n ($F_{i,n}$) then also depends on the frequencies of each genotype in the
278 patch and on the mate preferences of females computed in equation (13). We introduce the
preference coefficients $(Pref_{i,J})_{(i,J) \in \mathcal{G} \times \{A,B,C\}}$. These coefficients depend on the alleles at locus
280 M as detailed in the next section. For $(i, J) \in \mathcal{G} \times \{A, B, C\}$ the preference coefficient $Pref_{i,J}$ is
defined as $Pref_{i,J} = 1$ when females with genotype i accept males with phenotype J as mating
282 partners and $Pref_{i,J} = 0$ otherwise.

For $i \in \mathcal{G}, n \in \{1, 2\}$, we define $T_{i,n}$ as the probability that a female of genotype i in patch n
284 accepts a male during a mating encounter (see (Otto et al., 2008)):

$$T_{i,n} = Pref_{i,A}P_{A,n} + Pref_{i,B}P_{B,n} + Pref_{i,C}P_{C,n}, \quad (8)$$

where for $J \in \{A, B, C\}$, $P_{J,n} = \frac{\sum_{i \in \mathcal{G}} N_{i,n} \mathbb{1}_{\{CP(i)=J\}}}{\sum_{i \in \mathcal{G}} N_{i,n}}$ denotes the frequency of phenotype J in patch
286 n .

Because choosy individuals might have a reduced reproductive success due to limited mate
288 availability (Kirkpatrick and Nuismer, 2004; Otto et al., 2008), we also assume a relative fitness
cost associated with choosiness. This cost is modulated by the parameter c_r . When this cost is

290 absent ($c_r = 0$), females have access to a large quantity of potential mates, so that their mating
rate is not limited when they become choosy ("Animal" model). When this cost is high ($c_r = 1$),
292 females have access to a limited density of potential mates, so that their mating rate tends to
decrease when they become choosy ("Plant" model). Intermediate values of c_r implies that
294 females can partially recover the fitness loss due to the encountering of non-preferred males
towards reproduction with other males. This cost of choosiness is known to limit the evolution
296 of assortative mating (Otto et al., 2008) and may thus also limit the emergence of disassortative
mating.

298 Following (Otto et al., 2008) we compute the mating rate $M_{i,n}$ of a female with genotype i in
patch n :

$$M_{i,n} = 1 - c_r + c_r T_{i,n}. \quad (9)$$

300 We note \bar{M}_n the average mating rate in patch n defined as

$$\bar{M}_n = \sum_{i \in \mathcal{G}} f_{i,n} M_{i,n}, \quad (10)$$

where for $(i, n) \in \mathcal{G} \times \{1, 2\}$ $f_{i,n}$ is the frequency of genotype i in patch n .

302 For $(j, k) \in \mathcal{G}^2$, the quantity

$$\frac{f_{j,n} M_{j,n}}{\bar{M}_n}, \quad (11)$$

is the probability that, given that a female has mated in patch n , this female is of genotype j ,

304 and

$$\frac{Pref_{j,CP(k)} f_{k,n}}{T_{j,n}} = \frac{Pref_{j,CP(k)} f_{k,n}}{Pref_{j,A} P_{A,n} + Pref_{j,B} P_{B,n} + Pref_{j,C} P_{C,n}}, \quad (12)$$

is the probability that, given that a female of genotype j has mated in patch n , its mate is a
306 male of genotype k , depending on female preference and availability of males carrying genotype
 k .

308 For $(i, n) \in \mathcal{G} \times \{1, 2\}$, the frequency of genotype i in the progeny of the population living in patch n is

$$F_{i,n} = \sum_{(j,k) \in \mathcal{G}^2} \text{coef}(i, j, k, \rho) \times \underbrace{\frac{f_{j,n} M_{j,n}}{\bar{M}_n}}_{\text{probability, given that a female has mated, that this female is of genotype } j} \times \underbrace{\frac{\text{Pref}_{j,CP(k)} f_{k,n}}{T_{j,n}}}_{\text{probability, given that a female of genotype } j \text{ has mated, that her mate is a male of genotype } k}, \quad (13)$$

310 where $\text{coef}(i, j, k, \rho)$ controls the mendelian segregation of alleles during reproduction between an individual of genotype j and an individual of genotype k , depending on the recombination rate ρ between the color pattern locus P and the preference locus M (see Supp. S1 for
 312 detailed expression of $\text{coef}(i, j, k, \rho)$). We checked that for all n in $\{1, 2\}$ the sum of $F_{i,n}$ over all i
 314 is always equal to one, as expected (see Supp. S2).

Model exploration

316 The complexity of this two-locus diploid model prevents comprehensive exploration with analytical methods, we therefore used numerical simulations to identify the conditions promoting the
 318 evolution of disassortative mating. All parameters and parameter intervals used in the different simulations are summarized in Table 2. The values of the basic predation mortality factor d_m and
 320 d_{n-m} , the unpalatability λ and migration rate mig are chosen as conditions maintaining balanced polymorphism at the color pattern locus P **assuming random mating**, taken from (Joron and
 322 Iwasa, 2005).

Simulations are performed using Python v.3. and by using discrete time steps as an approximation (Euler method) (see Supp. S3 for more details about the numeric resolution). We checked
 324 that reducing the magnitude of the time step provided similar dynamics (see fig. S8), ensuring that our discrete-time simulations provide relevant outcomes. Note that all scripts used in this
 326 study are available on GitHub: [https://github.com/Ludovic-Maisonneuve/Evolution_and_](https://github.com/Ludovic-Maisonneuve/Evolution_and_genetic_architecture_of_disassortative_mating)
 328 [genetic_architecture_of_disassortative_mating](https://github.com/Ludovic-Maisonneuve/Evolution_and_genetic_architecture_of_disassortative_mating).

Abbreviation	Description
$N_{i,n}$	Density of individuals with genotype i in patch n
$Pred_{i,n}$	Change in the density of individuals with genotype i caused by to predation
$Rep_{i,n}$	Change in the density of individuals with genotype i caused by to reproduction
$Mig_{i,n}$	Change in the density of individuals with genotype i caused by to migration
$Mort_{i,n}$	Change in the density of individuals with genotype i caused by to mortality
$CP(i)$	Color pattern phenotype of individuals with genotype i
$Pref_{i,J}$	Preference of individuals with genotype i towards individuals with phenotype J
$f_{i,n}$	Frequency of genotype i in patch n
$P_{I,n}$	Frequency of phenotype I in patch n
$T_{i,n}$	Probability that a female of genotype i in patch n accepts a male as mating partner during one mating encounter
$M_{i,n}$	Mating rate of females with genotype i in patch n
\bar{M}_n	Average female mating rate in patch n
$F_{i,n}$	Frequency of genotype i in the progeny of the population living in patch n
P_{s-acc}	Proportion of individuals expressing a self-accepting behavior
P_{s-av}	Proportion of individuals expressing a self-avoidance behavior

Table 1: **Description of variables used in the model.**

Abbreviation	Description	Parameter interval
\mathcal{A}_P	Set of all possible alleles at locus P	$\{a, b, c\}$
\mathcal{A}_M	Set of all possible alleles at locus M	$\{r, sim, dis\}$ (hyp. 1) $\{m_r, m_a, m_b, m_c\}$ (hyp. 2)
\mathcal{G}	Set of all possible genotypes	$\mathcal{A}_P \times \mathcal{A}_P \times \mathcal{A}_M \times \mathcal{A}_M$
$N_{tot,n}^0$	Initial population density in patch n	100
d_m	Basic predation mortality factor for individuals displaying the color pattern matching the local community	0.05
d_{n-m}	Basic predation mortality factor for individuals displaying a color pattern different from the local community	0.15
λ	Unpalatability coefficient	0.0002
mig	Migration rate	[0,1]
ρ	Recombination rate	[0, 0.5]
r	Growth rate	1
K	Carrying capacity within each patch	2000
δ	Baseline mortality rate	0.1
δ_i	Genetic load linked to allele i	[0, 1]
c_r	Relative cost of choosiness	[0, 1]

Table 2: Description of parameters used in the model and range explored in simulations.

Introduction of preference alleles

330 We assume that random mating is the ancestral preference behavior. Before introducing prefer-
 332 ence alleles, we therefore introduce color pattern alleles in equal proportions, and let the pop-
 334 ulation evolves under random mating until the dynamical system reaches an equilibrium. We
 336 assume that a steady point is reached when the variation of genotype frequencies in the numer-
 338 ical solution during one time unit is below 10^{-5} (see Supp. S4 for more details). At this steady
 state, we then introduce the preference allele *dis* in proportion 0.01 (when exploring hyp. 1) or
 the preference alleles m_a, m_b, m_c in proportion $\frac{0.01}{3}$ (when exploring hyp. 2).

After the introduction of preference alleles, we follow the evolution of disassortative mating
 338 and its consequences in the two populations:

- Early dynamic : First, we identify the range of parameters enabling the emergence of
 340 disassortative mating, by tracking genotype numbers during the first 100 time steps after
 the introduction of preference alleles.
- Steady state : Then, we study the long-term evolutionary outcome associated with the
 342 changes in mating behavior, by computing genotype numbers at equilibrium, *i.e.* by run-
 344 ning simulations until the variation of genotype frequency during one time unit is below
 10^{-5} (see Supp. 4 for more details).

346 Summary statistics

To facilitate the interpretation of our results, we compute a number of summary statistics from the
 348 outcomes of our simulations. We define haplotypes as the pairs of alleles in $\mathcal{A}_P \times \mathcal{A}_M$ containing
 two alleles located on the same chromosome or inherited from the same parent. We then calculate
 350 haplotype frequencies in patch n ($f_{p,m,n}^{haplo}$) _{$(p,m) \in \mathcal{A}_P \times \mathcal{A}_M$} for $n \in \{1, 2\}$. Then for $(p, m, n) \in \mathcal{A}_P \times$
 $\mathcal{A}_M \times \{1, 2\}$, the frequency of haplotype (p, m) in patch n is given by:

$$f_{p,m,n}^{haplo} = \frac{\sum_{i=(p_m, p_f, m_m, m_f) \in \mathcal{G}} N_{i,n} (\frac{1}{2} \mathbb{1}_{\{p_m=p\}} \mathbb{1}_{\{m_m=m\}} + \frac{1}{2} \mathbb{1}_{\{p_f=p\}} \mathbb{1}_{\{m_f=m\}})}{\sum_{i=(p_m, p_f, m_m, m_f) \in \mathcal{G}} N_{i,n}}. \quad (14)$$

352 The estimation of haplotype frequencies allows to characterize the association between color
 pattern alleles and preference alleles, leading to different mating behaviors among partners with
 354 different color patterns, specifically under the *recognition/trait* hypothesis (Hyp.2). To characterize
 female mating preferences generated by the different genotypes at locus M and the link with their
 356 own color pattern phenotype, we then distinguish two main behaviors emerging under hyp. 2
 (fig. S6 and S7) for *attraction* (hyp. 2.a) and *rejection* (hyp. 2.b) hypotheses respectively:

- 358 • Self-acceptance : females mate with males displaying their own color pattern phenotype.
- Self-avoidance : females do not mate with males displaying their own color pattern pheno-
 360 type.

In order to compare the mating behaviors observed under *self-referencing* (hyp. 1) *attraction*
 362 (hyp. 2.a) and *rejection* (hyp. 2.b) hypotheses, we compute population statistics, P_{s-acc} (see equa-
 tion (15)) and P_{s-av} (see equation (16)) as the proportion of individuals exhibiting respectively
 364 a self-acceptance or a self-avoidance behavior throughout both patches. These two inferred be-
 haviors can be directly compared with mate preferences empirically estimated. For example,
 366 in experiments where females can choose partners among males displaying different color pat-
 terns (Chouteau et al., 2017), the proportion of females mating with males displaying their own
 368 phenotype color pattern can be easily scored and compared to the proportion of self-accepting
 individuals computed in our model.

370

$$P_{s-acc} = \sum_{i \in \mathcal{G}} f_i Pref_{i,CP(i)}, \quad (15)$$

$$P_{s-av} = \sum_{i \in \mathcal{G}} f_i (1 - Pref_{i,CP(i)}). \quad (16)$$

Results

Effect of mate choice on polymorphism

372

The emergence of disassortative mating requires initial polymorphism at the trait used as mating
374 cue. Because the costs associated with mate searching and courting penalize females preferring
rare phenotypes, the distribution of color pattern variation in the population may be an impor-
376 tant condition for the emergence of disassortative mating. In turn, the evolution of disassortative
mating is likely to generate a positive selection on rare phenotypes, therefore enhancing poly-
378 morphism at the color pattern locus P . To disentangle the feedbacks between polymorphism of
the cue and evolution of disassortative mating, we first investigate the impact of different mating
380 behaviors on the distribution of color pattern phenotypes within populations.

Under random mating, the frequencies of color pattern alleles at equilibrium computed for
382 different migration rates mig show that polymorphism can be maintained through an equilibrium
between spatially heterogeneous selection and migration (fig.1 (a)), consistent with previous re-
384 sults from the literature (Joron and Iwasa, 2005). In the absence of migration however, phenotypes
 A and B are fixed in the populations living in patch 1 and 2 respectively, owing to their mimetic
386 advantage within their respective communities. Polymorphism with persistence of phenotypes
 A and B within each population can only be maintained with migration, but in all cases the
388 non-mimetic phenotype C is not maintained in any of the two populations (fig.1 (a)).

To test for an effect of mate choice on this selection/migration equilibrium, we then com-
390 pare those simulations assuming random mating (*i.e.* with preference alleles r) with simulations
where *self-referencing* preference alleles generating either assortative (*sim* allele) or disassortative
392 (*dis* allele) behavior were introduced at the mate choice locus M (hyp. 1), assumed to be fully
linked to the color pattern locus P ($\rho = 0$). Assuming assortative mating via *self-referencing* (hyp.
394 1) the results are similar to those observed under random mating (fig.1 (a),(b)). Nevertheless,
the proportion of locally adapted alleles is higher than under random mating because assortative

396 mating reinforces positive frequency dependent selection on those alleles. In contrast, disassorta-
398 tive mating maintains a higher degree of polymorphism, with the two mimetic phenotypes A and
400 B and the non-mimetic phenotype C persisting within both populations, for all migration rates
(fig.1 (c)). The non-mimetic phenotype C is rarely expressed because allele c is recessive. Nev-
402 ertheless, individuals displaying phenotype C benefit from a high reproductive success caused
by disassortative mating. Indeed, the strict disassortative preference assumed here strongly in-
404 creases the reproductive success of individuals displaying a rare phenotype such as C . Negative
frequency-dependent selection (FDS hereafter) on color pattern thus generated by disassortative
406 mating counteracts the positive FDS due to predator behavior acting on the same trait. Therefore,
disassortative mate preferences can strongly promote polymorphism within the two populations
living in patch 1 and 2 respectively. When polymorphism is high, the cost of finding a dissimilar
mate may be reduced, therefore limiting selection against disassortative preferences. Our results
408 thus highlight the decreased cost of finding a dissimilar mate once disassortative mating becomes
established.

410 *Linked genetic load favors the persistence of maladaptive alleles*

In the following simulations, the migration parameter mig is set to 0.1, to allow for the persistence
412 of polymorphism of color pattern phenotype A and B when assuming random mating. We then
investigate the influence of a genetic load associated with the different color pattern alleles on
414 polymorphism at the color pattern locus P , under random mating. This allows quantifying
the effect of heterozygote advantage, independently of the evolution of mating preferences. We
416 observe that the non-mimetic phenotype C is maintained together with phenotypes A and B
within both populations, when (i) all three alleles carry a genetic load of similar strength, *i.e.*
418 $\delta_a = \delta_b = \delta_c > 0$ or (ii) when allele c is the only one without any associated genetic load
($\delta_a = \delta_b > 0$ and $\delta_c = 0$) (fig. S9). In contrast, phenotype C is not maintained when a genetic
420 load is associated with the non mimetic allele c only ($\delta_a = \delta_b = 0$ and $\delta_c > 0$), or when this load
is stronger than the one associated with alleles a and b (fig. S9). The heterozygote advantage

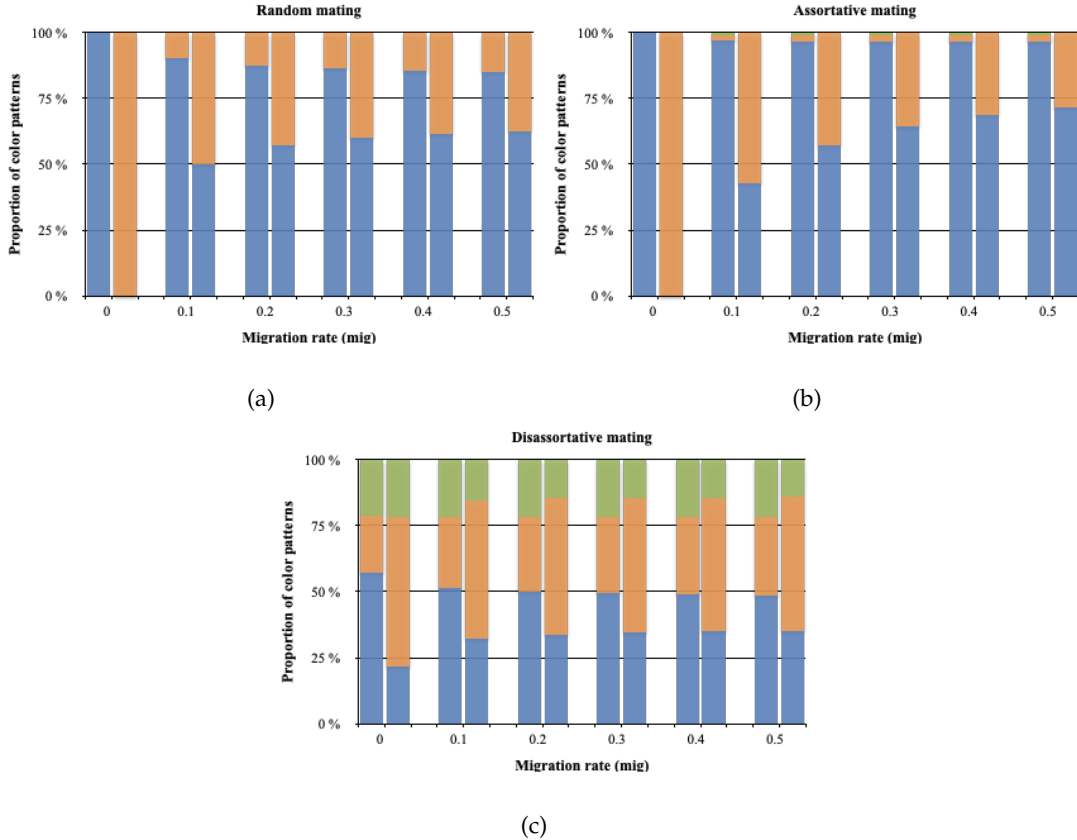


Figure 1: **Influence of mate preferences on color pattern diversity within both patches.** The equilibrium frequencies of color pattern phenotypes in patches 1 and 2 for different migration rates mig are computed assuming different mating behaviors, *i.e.*, random (a), assortative (b) or disassortative (c). The heights of the colored stacked bars indicate the frequencies of color pattern phenotypes A , B and C (blue, orange and green areas respectively) in patches 1 and 2 (on the left and right side respectively, for each migration level). The three alleles at the locus P controlling color pattern variations are introduced in proportion $\frac{1}{3}$ in each patch. The locus M controls for the *self-referencing* based mate preferences (hyp. 1): preferences alleles r , sim and dis were introduced in simulations shown in panel (a), (b) and (c) respectively. Simulations are run assuming $r = 1$, $K = 2000$, $N_{tot,1}^0 = N_{tot,2}^0 = 100$, $\lambda = 0.0002$, $d_m = 0.05$, $d_{n-m} = 0.15$, $\rho = 0$, $c_r = 0.1$, $\delta_a = \delta_b = \delta_c = 0$ and $\delta = 0.1$.

422 generated by genetic load associated with the dominant mimetic alleles at locus P therefore favors
the persistence of a balanced polymorphism and more specifically promotes the maintenance of
424 allele c in both patches, even though this allele does not bring any benefit through local (mimicry)
adaptation.

Evolution of disassortative mating

426

Because we expect heterozygote advantage at the color pattern locus P to enhance the evolu-
428 tion of disassortative mating preferences at locus M , we first investigate the influence of a genetic
load on the evolution of disassortative behavior by testing the invasion of *self-referencing* mutation
430 triggering self-avoidance *dis* (hyp. 1) in a population initially performing random mating with
genotype frequencies at equilibrium. We compute the frequency of mutants 100 time units after
432 their introduction, assuming full linkage between loci P and M . Figure 2 shows that the genetic
load associated with alleles a and b ($\delta_a = \delta_b$), has a strong positive impact on the emergence of
434 disassortative mating. The genetic load associated with the recessive allele c (δ_c) has a weaker
positive effect on the evolution of disassortative mating. Simulations assuming different relative
436 cost of choosiness (c_r) show a similar effect of associated genetic loads (see fig. 2). However the
cost of choosiness reduces the range of genetic load values allowing the emergence of disassorta-
438 tive preference. When this cost is high, the invasion of mutant allele *dis* is prevented, regardless
of the strength of genetic load (see fig. 2(d)). Although an increased cost of choosiness slows
440 down the invasion of the disassortative mating mutant *dis* (see fig. 2), a genetic load linked to the
color pattern locus P generally favors the emergence of disassortative mating in both patches.

442 To investigate the long-term evolution of disassortative mating promoted by the genetic loads
associated with color pattern alleles, we then compute the frequency of mutant allele *dis* at
444 equilibrium in conditions previously shown to promote its emergence (*i.e.* assuming limited
cost of choosiness). Figure 3 shows that the mutant preference allele *dis* is never fixed within
446 populations. This suggests that the heterozygote advantage at locus P allowing the emergence of
disassortative mating decreases when this behavior is common in the population. The *dis* mutant
448 nevertheless reaches high frequencies when the genetic load associated with the recessive allele c
is intermediate ($\delta_c \approx 0.35$) and the genetic load associated with dominant alleles a and b is strong
450 (see fig. 3). This result seems surprising because the highest level of disassortative mating is not
reached when the genetic load is at the highest in all the three alleles at locus P . On the contrary,

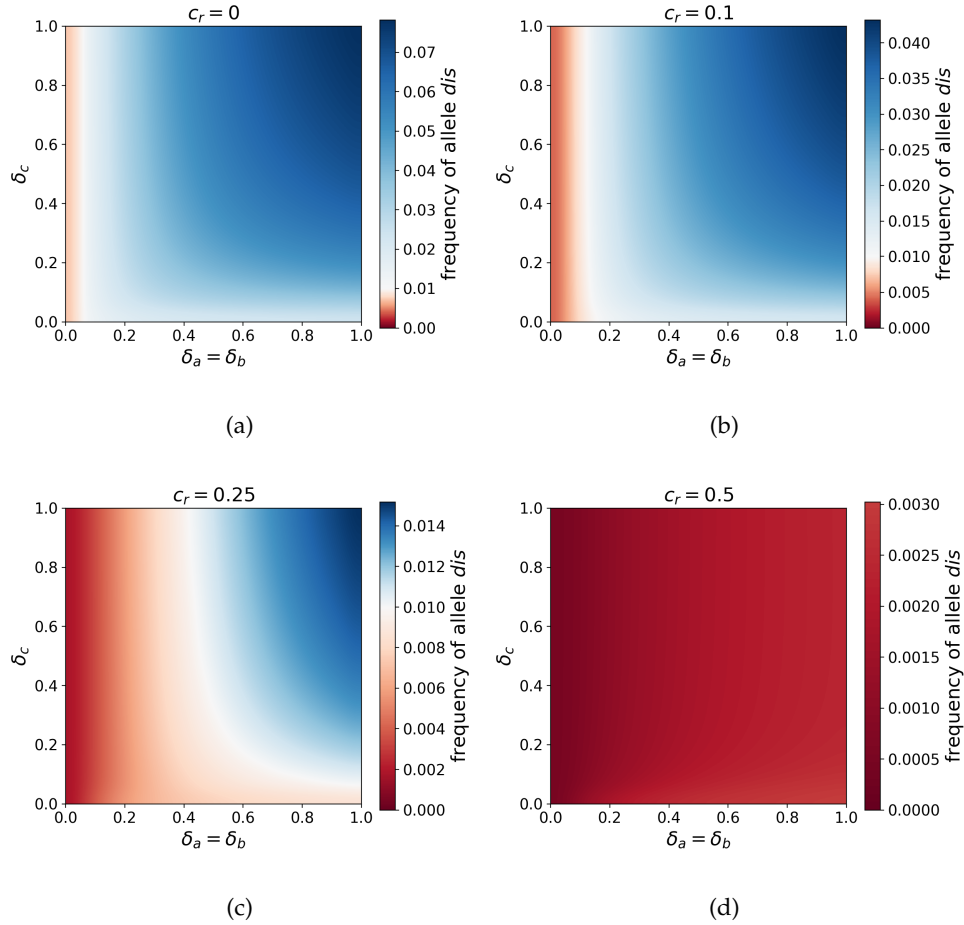


Figure 2: **Influence of a linked genetic load on the emergence of disassortative mating for different costs of choosiness, assuming *self-referencing* (hyp. 1).** The frequency of the mutant allele *dis* is shown 100 time units after its introduction depending on the strength of genetic load associated with the dominant alleles a and b ($\delta_a = \delta_b$) and to the recessive allele c , δ_c . The initial frequency of allele *dis* was 0.01, the area where mutant allele increase (resp. decrease) is shown in blue (resp. red). Simulations are run assuming either (a) no cost of choosiness $c_r = 0$, (b) a low cost of choosiness $c_r = 0.1$, (c) an intermediate cost of choosiness $c_r = 0.25$ or (d) an elevated cost of choosiness $c_r = 0.5$. Simulations are run assuming $r = 1$, $K = 2000$, $N_{tot,1}^0 = N_{tot,2}^0 = 100$, $\lambda = 0.0002$, $d_m = 0.05$, $d_{n-m} = 0.15$, $mig = 0.1$ and $\rho = 0$.

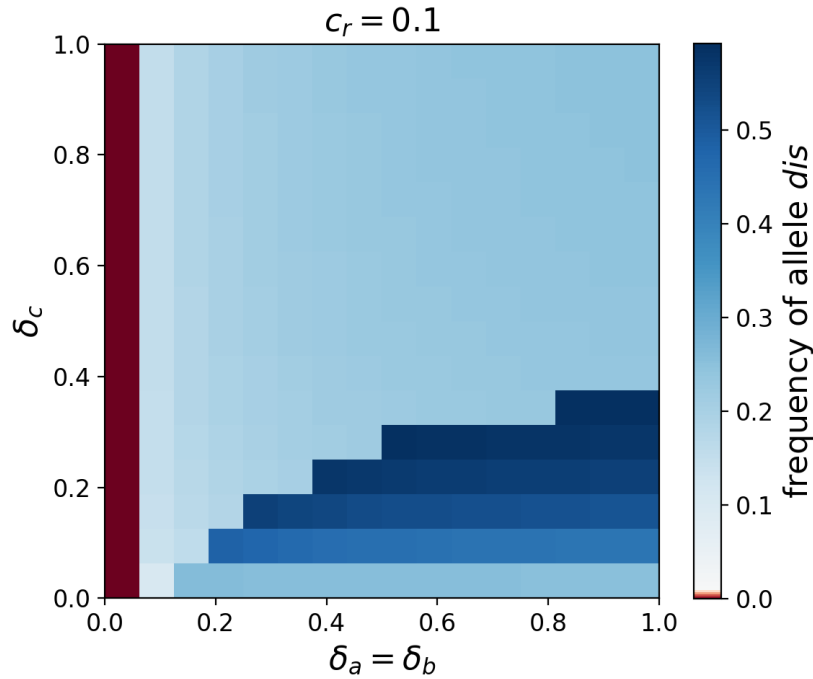


Figure 3: Influence of a linked genetic load on the level of disassortative mating at equilibrium for low cost of choosiness ($c_r = 0.1$), assuming *self-referencing* (hyp. 1). The frequency of the mutant allele *dis* is shown at equilibrium after its introduction depending on the strength of genetic load associated with the dominant alleles *a* and *b* ($\delta_a = \delta_b$) and with the recessive allele *c*, δ_c . The initial frequency of allele *dis* is 0.01. The area where the frequency of the mutant allele increases (resp. decrease) is shown in blue (resp. red). Simulations are run assuming $r = 1$, $K = 2000$, $N_{tot,1}^0 = N_{tot,2}^0 = 100$, $\lambda = 0.0002$, $d_m = 0.05$, $d_{n-m} = 0.15$, $mig = 0.1$, $\rho = 0$ and $c_r = 0.1$.

452 disassortative mating is favoured when a genetic load is associated with the dominant alleles
only: disassortative mating limits more the cost of producing unfit offspring when a genetic load
454 is associated with dominant alleles, because these alleles are always expressed as color pattern
phenotypes, and therefore avoided by females with disassortative preferences.

456 *How does the genetic architecture of mating preference influence the evolution of*
457 *disassortative mating ?*

458 To study the impact of the genetic architecture of mate preferences on the evolution of disas-
sortative mating, we then compare the invasion of *self-referencing* alleles *dis* with the invasion
460 of *recognition/trait* alleles (*i.e.* alleles m_r , m_a , m_b and m_c controlling random mating and specific
recognition of phenotype *A*, *B* and *C* respectively, hyp. 2). We assume loci *P* and *M* to be fully
462 linked ($\rho = 0$), and compare simulations where mate preference alleles trigger either disassorta-
tive preference (hyp. 1), *attraction* (hyp. 2.a) or *rejection* (hyp. 2.b) of the recognized color pattern
464 phenotype. We report the frequencies of haplotypes, in order to follow the association of color
pattern and preference alleles (fig.4(a), fig.4(b) and fig.4(c) respectively).

466 Under a *self-referencing* rule, alleles *a* and *b* are associated with preference allele *dis* as soon as
the genetic load associated with the dominant alleles (alleles *a* and *b*) is greater than 0. Indeed
468 disassortative mating favors the production of heterozygotes and reduces the expression of the
genetic load in the offspring. In contrast, the non-mimetic allele *c*, not associated with any genetic
470 load, is preferentially linked with the random mating allele *r*. **This result is surprising because**
heterozygotes carrying a *c* allele have a lower predation risk than homozygotes with two *c* alleles:
472 **homozygotes are indeed non-mimetic in both patches, while heterozygotes are mimetic in one**
out of the two patches. However, the benefit associated with haplotype (*c, dis*) through increased
474 **production of heterozygous offspring is weak. Because of the genetic load associated with the**
dominant color alleles *a* and *b*, *c* allele is common in the population, resulting in relatively high
476 **frequency of homozygotes with two *c* alleles, and of heterozygotes with one *c* allele. Alleles *a***
and *b* are frequently linked with the disassortative preference allele *dis*, further promoting the
478 **formation of heterozygotes. Since *c* allele is recessive, disassortative crosses between individuals**
with phenotype *C* and either *A* or *B* then frequently produce progeny with half of the offspring
480 **carrying two *c* alleles, suffering from increased predation. The limited survival of these offspring**
reduces the benefits associated with the haplotype (*c, dis*). Because the *dis* allele is also associated

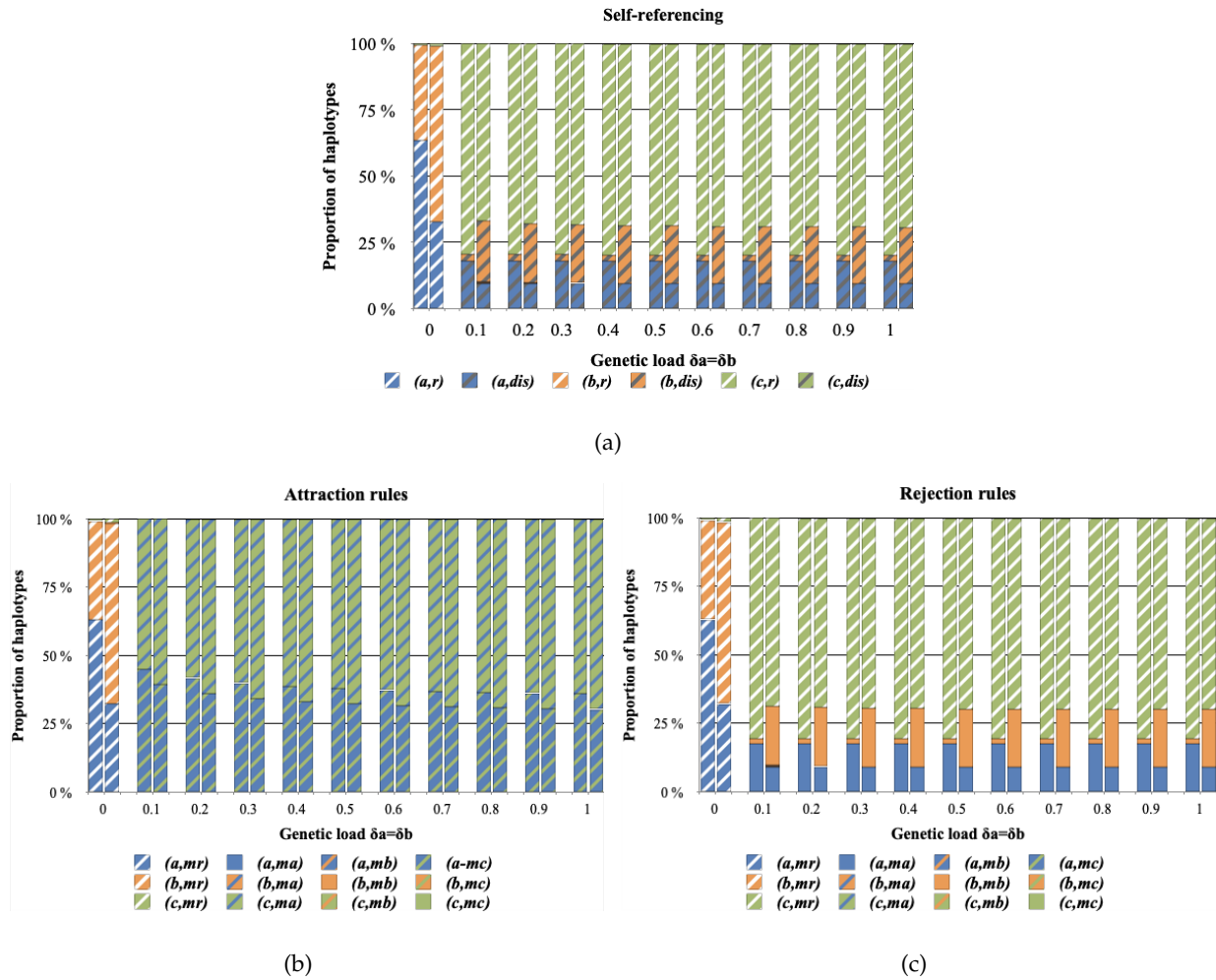


Figure 4: Influence of a genetic load on haplotype diversity, assuming (a) *self-referencing* (hyp. 1), (b) *attraction rule* (hyp. 2.a) or (c) *rejection rule* (hyp. 2.b) at the preference locus (*recognition/trait*). The proportion of haplotypes at equilibrium after the introduction of preference alleles in both patches are shown for different values of genetic load associated with alleles *a* and *b* ($\delta_a = \delta_b$). For each value of genetic load ($\delta_a = \delta_b$) the first and second bars show the frequencies of haplotypes in the patches 1 and 2 respectively. Simulations are run assuming $r = 1$, $K = 2000$, $N_{tot,1}^0 = N_{tot,2}^0 = 100$, $\lambda = 0.0002$, $d_m = 0.05$, $d_{n-m} = 0.15$, $\rho = 0$, $mig = 0.1$, $\delta_c = 0$, $\delta = 0.1$ and $c_r = 0.1$.

482 with a cost of choosiness, linkage between allele *c* and the random mating allele *r* could then be promoted.

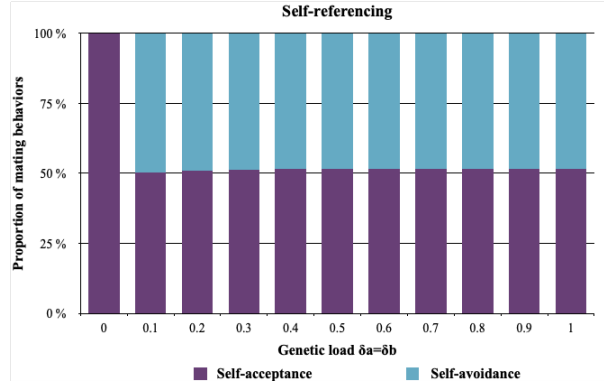
484 When preference alleles cause female attraction to males exhibiting a given phenotype (hyp. 2.a), only haplotypes (*a, m_c*) and (*c, m_a*) are maintained in both patches at equilibrium (fig.4(b)).

486 The haplotype (a, m_c) benefits from both positive selection associated with mimicry and limited
expression of the genetic load due to the preferential formation of heterozygotes. Haplotype
488 (c, m_a) is maintained because of the benefit associated with the choice of the most frequent
mimetic phenotype A , and the limited expression of the non-mimetic phenotype C due to c being
490 recessive. The proportion of haplotype (a, m_c) decreases as the genetic load associated with allele
 a increases. Indeed the mating between two individuals of genotype (a, c, m_c, m_a) becomes more
492 likely and leads to the formation of individuals (a, a, m_c, m_c) suffering from the expression of
the genetic load. Allele b is then lost because of the dominance relationships between alleles a
494 and b . Phenotype A is more commonly expressed than phenotype B : haplotype (c, m_a) is thus
favoured over haplotype (c, m_b) , through increased mate availability. Sexual selection caused
496 by disassortative preferences generate a strong disadvantage associate with b allele, ultimately
leading to its extinction.

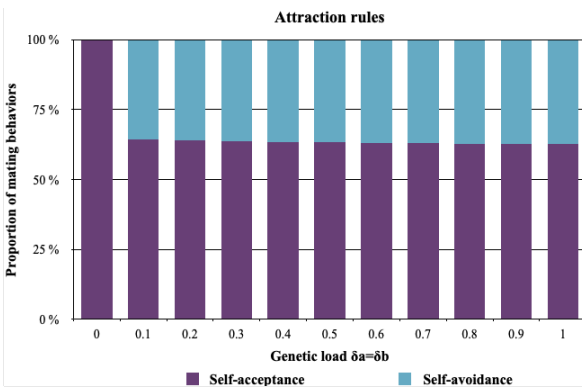
498 By contrast, when mate preference is based on alleles causing *rejection* behavior (hyp. 2.b) and
when a genetic load is associated with the mimetic alleles a and b at locus P , these alleles become
500 associated with the corresponding rejection alleles at locus M (i.e. (a, m_a) and (b, m_b) have an
intermediate frequencies in both patches) (fig.4(c)). Non mimetic allele c becomes associated
502 with random mating preference allele r . The three alleles (a , b and c) persist within patches for
all positive values of genetic load. This contrasts with the evolutionary outcome observed under
504 attraction rule (hyp. 2.a) where mimetic allele b is lost if the genetic load is greater than 0 (fig.
4(b)).

506 We then investigate how these haplotype frequencies translate into individual behaviors in
the populations at equilibrium. As highlighted in fig.5, the proportion of each behavior de-
508 pends more on the existence of a genetic load linked to dominant alleles, than on its strength.
The proportion of disassortative mating is similar when assuming *self-referencing* (hyp. 1) and
510 *recognition/trait* leading to rejection (hyp. 2.b) ($P_{s-av} \approx 48\%$) (fig.5(a) and 5(c)).

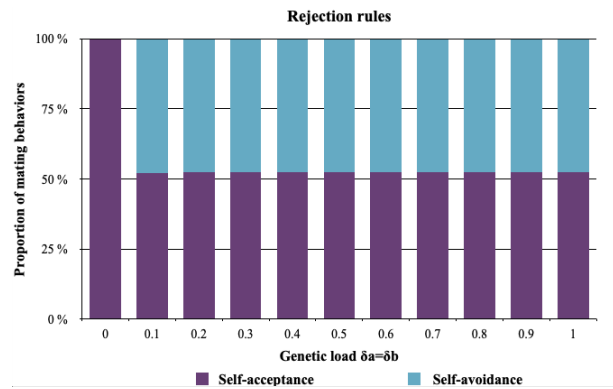
By contrast, when we consider preference alleles leading to *attraction* (hyp. 2.a), the disassor-
512 tative behavior is scarcer at equilibrium ($P_{s-av} \approx 36\%$) (fig. 5(b)). This may seem surprising given



(a)



(b)



(c)

Figure 5: Influence of a genetic load on the distribution of mating behavior observed at the population level, assuming (a) *self-referencing* (hyp. 1), (b) *attraction rule* (hyp. 2.a) or (c) *rejection rule* (hyp. 2.b) at the preference locus (*recognition/trait*). The proportion of individuals displaying self-acceptance P_{s-acc} (in purple) and self-avoidance P_{s-av} (in blue) obtained at equilibrium after the introduction of preference alleles are shown for different values of the level of genetic load of δ_a and δ_b . Simulations are run assuming $r = 1$, $K = 2000$, $N_{tot,1}^0 = N_{tot,2}^0 = 100$, $\lambda = 0.0002$, $d_m = 0.05$, $d_{n-m} = 0.15$, $\rho = 0$, $mig = 0.1$, $\delta_c = 0$, $\delta = 0.1$ and $c_r = 0.1$.

514 that most haplotypes are formed by a color pattern allele linked with an *attraction* allele for a
 516 different color pattern (fig. 4(b)). Nevertheless, the color pattern allele c is linked to m_a coding
 for attraction to A . As a consequence, most individuals formed are heterozygous at both the
 color pattern locus P (with one allele a and one allele c) and at the preference locus M (with one
 preference allele coding for attraction toward phenotype A and another preference allele trig-

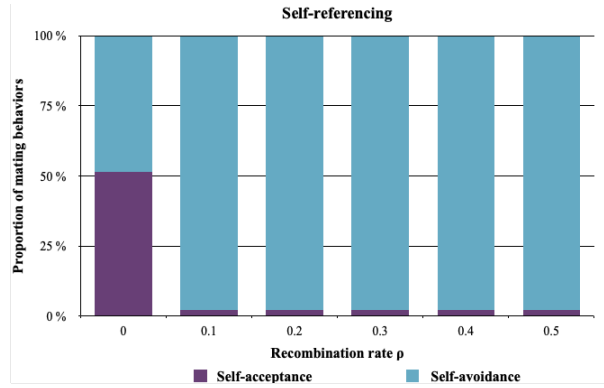
518 gering attraction toward phenotype C). These double heterozygotes thus benefit from mimicry
and avoid the expression of deleterious mutations, and are self-accepting. However, under the
520 *self-referencing* (hyp. 1) or *rejection* (hyp. 2.b) rules disassortative mating is more likely to emerge.
Indeed under hyp. 2.b, haplotypes composed by a phenotype allele and its corresponding pref-
522 erence allele ((a, m_a) for example) generally immediately translates into a self-avoiding behavior,
whatever the genotypic combinations within individuals. Moreover under hyp. 1 disassortative
524 haplotype, *i.e.* an haplotype where the preference allele is *dis*, always generates a disassortative
behavior.

526 This highlights that the genetic architecture of mate preference plays a key role in the evo-
lution of the mating behavior of diploid individuals: the evolution of disassortative haplotypes
528 inducing disassortative preferences do not necessarily cause disassortative mating at the popu-
lation level. At equilibrium, the proportion of self-avoidance behavior in the population hardly
530 depends of the strength of the genetic load (figure 5). However, the strength of the genetic load
does **increase** the speed of evolution of disassortative mating (see fig. S10 **comparing the invasion**
532 **dynamics of the self-avoiding behavior when assuming different levels of genetic load**), therefore
suggesting stronger positive selection on disassortative mating when the genetic load associated
534 with dominant wing color pattern alleles is higher.

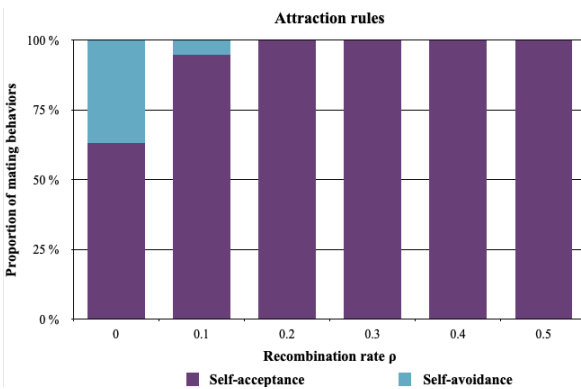
Impact of linkage between loci P and M on the evolution of disassortative mating

536 In previous sections, we observed that the genetic load associated with the two most dominant
alleles at the color pattern locus *P* impacts the evolution of mate choice. **Assuming that the color**
538 **pattern locus P and the preference locus M are fully linked, we also noticed** that disassortative
mating **is more prevalent at equilibrium under** the *self-referencing* rule (hyp. 1) and the *rejection*
540 **rule** (hyp. 2.b) **rather than under the attraction** (hyp. 2.a) rule. We then test for an effect of
recombination between alleles at the two loci on the evolution of mate choice by performing
542 simulations with different values of the recombination rate ρ .

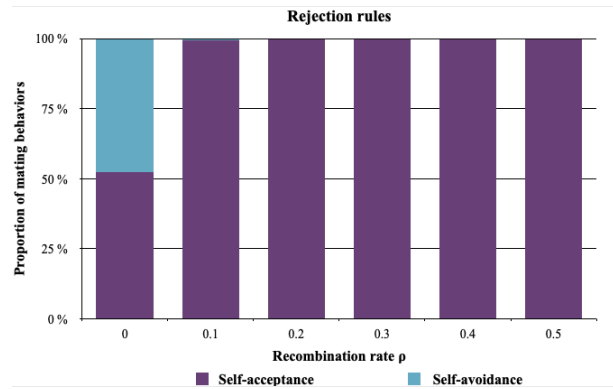
Assuming *self-referencing* (hyp. 1), increasing recombination rate strongly promotes the self-



(a)



(b)



(c)

Figure 6: Influence of the recombination rate between color pattern and preference alleles on the distribution of mating behavior observed at the population level, assuming different genetic architectures of mate preferences: either (a) *self-referencing* (hyp. 1), or *recognition/trait* leading to (b) *attraction rule* (hyp. 2.a) or (c) *rejection rule* (hyp. 2.b). The proportion of individuals displaying self-acceptance P_{s-acc} (in purple) and self-avoidance P_{s-av} (in blue) obtained at equilibrium are shown for different values of recombination rate ρ between the preference locus M and the color pattern locus P . Simulations are run assuming $r = 1$, $K = 2000$, $N_{tot,1}^0 = N_{tot,2}^0 = 100$, $\lambda = 0.0002$, $d_m = 0.05$, $d_{n-m} = 0.15$, $mig = 0.1$, $\delta_a = \delta_b = 0.5$, $\delta_c = 0$, $\delta = 0.1$ and $c_r = 0.1$.

544 avoidance behavior ($P_{s-av} \approx 98\%$) (see fig. 6(a)). Selection generated by the genetic load associated
to color pattern alleles a and b promotes their linkage with the disassortative *self-referencing* allele
546 dis , while the genetic-load free allele c tends to be linked to the random mating allele r (as
observed in simulations assuming no recombination, fig. S11(a)). Because allele dis reaches
548 a high frequency in the population, recombination generates a large density of recombinant

haplotypes (a, r) , (b, r) , (c, dis) . Haplotypes (a, r) and (b, r) are disfavored because they lead to a
550 the production of offspring suffering from the expression of a genetic load, whereas (c, dis) leads
to the production of viable offspring. Therefore, under the *self-referencing* hypothesis (hyp. 1),
552 recombination thus significantly increases the proportion of disassortative mating.

Under *self-referencing* rule (hyp. 1), mate preference depends on the phenotype displayed by
554 the individual, so that allele *dis* always translates into a disassortative behavior. By contrast, when
assuming *recognition/trait* for a given color pattern allele (hyp. 2), mating behavior depends only
556 on the genotype at the preference locus M , independently from the color pattern of the female.
We therefore expect a stronger effect of recombination rate on mate choice evolution. Figure 6
558 indeed confirms this prediction. Under *attraction* (hyp. 2.a) and *rejection* (hyp. 2.a) rules, the most
striking effect is observed when comparing simulations assuming $\rho = 0$ vs $\rho > 0$: self-avoidance
560 behavior is scarcely observed in the population ($P_{s-av} \approx 1\%$) when there is recombination ($\rho > 0$).

Our results suggest that disassortative mating can emerge either (1) under the *self-referencing*
562 rule or (2) under the *recognition/trait* rule assuming a tight linkage between the loci controlling
cue and preference. Nevertheless, strict *self-referencing* behaviour, under which preference varies
564 according to the chooser's phenotype, is scarcely observed in natural populations (see Kopp et al.
(2018) for a review). We thus expect that disassortative mating might emerge when the mating
566 cue and the preference loci are tightly linked or are controlled by a single pleiotropic gene.

Discussion

568 *Genetic architecture of disassortative mating: theoretical predictions*

Our model shows that without recombination between color pattern (locus P) and preference
570 alleles (locus M), disassortative mating is more likely to emerge when the genetic architecture is
with *self-referencing* (hyp. 1) or with color pattern recognition triggering *rejection* (hyp. 2.b). When
572 preference alleles cause *attraction* to males exhibiting a given phenotype (hyp. 2.a), heterozygote
advantage favors haplotypes formed by a color pattern allele linked with an attraction allele

574 for a different color pattern. However, these haplotypes do not necessarily imply a complete
self-avoidance behavior in females carrying them. The co-dominance assumed at the preference
576 locus indeed generates preference for two different phenotypes in heterozygotes at the locus M ,
favoring self-acceptance. This effect is reinforced by the mate choice, promoting the association
578 between a color allele and the corresponding attraction allele in the offspring, and therefore in-
creasing the emergence of self-accepting genotypes. This might explain the low proportion of
580 self-avoidance behavior observed within populations, when assuming the *attraction* rule (hyp.
2.a). By contrast, when recombination between the two loci does occur, a *self-referencing* ar-
582 chitecture (hyp. 1) may facilitate the evolution of disassortative mating. The genetic basis of
disassortative mating is largely unknown in natural populations. Assortative mating is better
584 documented, for instance in *Heliconius* butterflies where it is generally associated with attraction
towards a specific cue. The locus controlling preference for yellow *vs.* white in *H. cydno* maps
586 close to the gene *aristalless*, whose expression differences determine the white/yellow switch in
this species (Kronforst et al., 2006; Westerman et al., 2018). In *H. melpomene*, a major QTL associ-
588 ated with preference towards red was identified in crosses between individuals displaying a red
pattern and individuals with a white pattern (Merrill et al., 2019). This QTL is also located close
590 to the gene *optix* involved in the variation of red patterning in *H. melpomene*. Assortative mating
in *Heliconius* thus seems to rely on alleles encoding preference for specific cues, linked to with
592 loci involved in the variation of these cues. Similarly, our model suggests that the genetic archi-
tecture of disassortative mating might involve tight linkage between the cue and the preference
594 loci. However, in contrast with the attraction alleles documented in species where assortative
mating behavior is observed, our results show that alleles coding for rejection toward certain cue
596 are more likely to promote the evolution of disassortative mating.

Similar mate preference is obtained with some *recognition/trait* (hyp.2) genotypes than with
598 some *self-referencing* (hyp. 1) genotypes: for example, under the *rejection* rule (hyp. 2.b), the
genotype (a, a, m_a, m_a) leads to the same mate preference as the genotype (a, a, dis, dis) under the
600 *self-referencing* genetic architecture. Introducing recombination in the *recognition/trait* architecture

then enables the decoupling of the mating cue and of its corresponding preference alleles, thereby
602 disrupting the self rejection behavior. Furthermore, under the *recognition/trait* architecture, our
model distinguishes whether the specific recognition of the cue leads to *rejection* or *attraction*, and
604 highlights that these two hypotheses lead to the evolution of different preference regimes: disas-
sortative mating is more likely to emerge assuming a *rejection rule*. This rule indeed generates a
606 greater density of self-rejecting haplotypes than the *attraction rule*, although recombination limits
this effect.

608 *The dominance relationships assumed at both the cue and preference loci are likely to impact
our predictions on the evolution of disassortative mating. Disassortative mating at an advantage
when it favors the production of offspring that do not express the genetic load. Dominance
relationships at the color pattern locus *P* signal the genetic load associated with dominant cue
610 alleles. This explains why disassortative mating is favored when the genetic load is low in
the recessive cue alleles and large in dominant cue alleles. The co-dominance assumed at the
612 preference locus generates preferences toward two different phenotypes in heterozygotes at the
preference locus. We suspect that alternative hypotheses on dominance at the preference locus
614 may modulate our predictions on the evolution of disassortative mating.*

Altogether, our theoretical model shows that the genetic basis of mate preferences has a
618 strong impact on the evolution of disassortative mating at loci under heterozygote advantage.
This emphasizes the need to characterize the genetic basis of mate preference empirically and
620 the linkage disequilibrium with the locus controlling variation in the mating cues.

*Evolution of disassortative mating results from interactions between dominance
622 and deleterious mutations*

Here, we confirm that the evolution of disassortative mating is promoted by the heterozygote ad-
624 vantage associated with alleles determining the mating cue. As mentioned above, the phenotype
of the chosen individuals depends on the dominance relationships at the color pattern locus.

626 Our model highlights that a genetic load associated with the dominant alleles contributes more
to disassortative mating than a genetic load associated with the most recessive haplotype. This
628 theoretical prediction is in accordance with the few documented cases of polymorphism pro-
moted by disassortative mating. In the polymorphic butterfly *Heliconius numata* for instance, the
630 top dominant haplotype *bicoloratus* is associated with a strong genetic load (Jay et al., 2019). Simi-
larly, in the white throated sparrow, the dominant *white* allele is also associated with a significant
632 genetic load (Tuttle et al., 2016). Again, in the self-incompatibility locus of the *Brassicaceae*, dom-
inant haplotypes carry a higher genetic load than recessive haplotypes (Llaurens et al., 2009).
634 Disassortative mating is beneficial because it increases the number of heterozygous offspring
with higher fitness. Once disassortative mating is established within a population, recessive
636 deleterious mutations associated with the dominant haplotype become sheltered because the for-
mation of homozygotes carrying two dominant alleles is strongly reduced, thereby limiting the
638 opportunities for purging via recombination (Llaurens et al., 2009). Falk and Li (1969) proved
that disassortative mate choice promotes polymorphism, and therefore limits the loss of alleles
640 under negative selection. Disassortative mating might thus shelter deleterious mutations linked
to dominant alleles, and reinforce heterozygote advantage. The sheltering of deleterious muta-
642 tions is favored by the interaction between two aspects of the genetic architecture: dominance at
the mating cue locus and limited recombination. This is likely to happen in polymorphic traits
644 involving chromosomal rearrangements, where recombination is limited. Many rearranged hap-
lotypes are indeed associated with serious fitness reduction as homozygotes (Faria et al., 2019),
646 such as in the derived haplotypes of the supergene controlling plumage and mate preferences
in the white-throated sparrow (Thomas et al., 2008). The deleterious elements in the inverted
648 segment can be due to an initial capture by the inversions (Kirkpatrick, 2010), but they could
also accumulate through time, resulting in different series of deleterious mutations associated to
650 inverted and non-inverted haplotypes (Berdan et al., 2019).

Here, we assume that mate choice relied purely on a single cue. Nevertheless, mate choice
652 could be based on other cues, controlled by linked loci and enabling discrimination between

homozygotes and heterozygotes, thereby further increasing the proportion of heterozygous off-
654 springs with high fitness. We also modelled strict preferences regarding color patterns, but
choosiness might be less stringent in the wild, and may limit the evolution of disassortative
656 mating. Depending on the cues and dominance relationships among haplotypes, different mate
choice behaviors may also evolve, which might modulate the evolution of polymorphism within
658 populations. Our model thus stresses the need to document dominance relationships among
haplotypes segregating at polymorphic loci, as well as mate choice behavior and cues, to under-
660 stand the evolutionary forces involved in the emergence of disassortative mating.

Conclusions

662 Inspired by a well-documented case of disassortative mating based on cues subject to natural
selection, our model shows that heterozygote advantage is likely to favor the evolution of disas-
664 sortative mating preferences. We highlight that disassortative mating is more likely to emerge
when loci code for self-referencing disassortative preference or rejection of specific cues. How-
666 ever rejection locus only promotes disassortative mating when they are in tight linkage with the
locus controlling mating cue variation.

Acknowledgments

668 The authors would like to thank Charline Smadi and Emmanuelle Porcher for feedbacks on the
670 modeling approach developed here. We also thank Thomas Aubier and Richard Merrill and
the whole *Heliconius* group for stimulating discussion on mate choice evolution in our favorite
672 butterflies. We are also grateful to Roger Butlin, Charles Mullan, Tom Van Dooren and two
anonymous reviewers for their thoughtful review of a previous versions of this manuscript.
674 We also thank Sylvain Gerber for his help in improving the English of this article. This work
was supported by the Emergence program from Paris City Council to VL and the ANR grant
676 SUPERGENE to VL and MJ.

Conflict of interest disclosure

678 The authors of this preprint declare that they have no financial conflict of interest with the content
of this article. Violaine Llaurens and Mathieu Joron are listed as PCI Evol Biol recommenders.

References

- 680
- M. Arias, A. Meichanetzoglou, M. Elias, N. Rosser, D. L. De-Silva, B. Nay, and V. Llaurens.
682 Variation in cyanogenic compounds concentration within a heliconius butterfly community:
does mimicry explain everything? BMC evolutionary biology, 16(1):272, 2016.
- 684 E. L. Berdan, A. Blanckaert, R. K. Butlin, and C. Bank. Muller’s ratchet and the
long-term fate of chromosomal inversions. bioRxiv, 2019. 10.1101/606012. URL
686 <https://www.biorxiv.org/content/early/2019/04/13/606012>.
- R. K. Butlin, P. M. Collins, and T. H. Day. The effect of larval density on an inversion polymor-
688 phism in the seaweed fly *Coelopa frigida*. Heredity, 1984.
- L. Casselton. Mate recognition in fungi. Heredity, 88(2):142, 2002.
- 690 M. Chouteau, M. Arias, and M. Joron. Warning signals are under positive
frequency-dependent selection in nature. Proceedings of the National Academy of
692 Sciences, 113(8):2164–2169, 2016a. ISSN 0027-8424. 10.1073/pnas.1519216113. URL
<https://www.pnas.org/content/113/8/2164>.
- 694 M. Chouteau, M. Arias, and M. Joron. Warning signals are under positive frequency-dependent
selection in nature. Proceedings of the national Academy of Sciences, 113(8):2164–2169, 2016b.
- 696 M. Chouteau, V. Llaurens, F. Piron-Prunier, and M. Joron. Polymorphism at a mimicry supergene
maintained by opposing frequency-dependent selection pressures. Proceedings of the National
698 Academy of Sciences, 114(31):8325–8329, 2017.

- M. Chouteau, J. Dezeure, T. N. Sherratt, V. Llaurens, and M. Joron. Similar predator aversion for natural prey with diverse toxicity levels. Animal Behaviour, 153: 49 – 59, 2019. ISSN 0003-3472. <https://doi.org/10.1016/j.anbehav.2019.04.017>. URL <http://www.sciencedirect.com/science/article/pii/S000334721930137X>.
- T. H. Day and Butlin. Non-random mating in natural populations of the seaweed fly, *Coelopa frigida*. Heredity, 1987.
- M. de Cara, N. Barton, and M. Kirkpatrick. A model for the evolution of assortative mating. The American Naturalist, 171(5):580–596, 2008. 10.1086/587062. URL <https://doi.org/10.1086/587062>. PMID: 18419568.
- C. T. Falk and C. C. Li. Negative assortative mating: Exact solution to a simple model. Genetics, 1969.
- R. Faria, K. Johannesson, R. K. Butlin, and A. M. Westram. Evolving inversions. Trends in ecology & evolution, 2019.
- S. J. Hiscock and S. M. McInnis. Pollen recognition and rejection during the sporophytic self-incompatibility response: Brassica and beyond. Trends in plant science, 8(12):606–613, 2003.
- R. D. Holt. Population dynamics in two-patch environments: Some anomalous consequences of an optimal habitat distribution. Theoretical Population Biology, 28(2): 181 – 208, 1985. ISSN 0040-5809. [https://doi.org/10.1016/0040-5809\(85\)90027-9](https://doi.org/10.1016/0040-5809(85)90027-9). URL <http://www.sciencedirect.com/science/article/pii/0040580985900279>.
- B. M. Horton, Y. Hu, C. L. Martin, B. P. Bunke, B. S. Matthews, I. T. Moore, J. W. Thomas, and D. L. Maney. Behavioral characterization of a white-throated sparrow homozygous for the *zal2* m chromosomal rearrangement. Behavior genetics, 43(1):60–70, 2013.
- A. M. Houtman and J. B. Falls. Negative assortative mating in the white-throated sparrow,

722 zonorhina albicollis: the role of mate choice and intra-sexual competition. Animal Behaviour,
48(2):377–383, 1994.

724 P. Jay, M. Chouteau, A. Whibley, H. Bastide, V. Llaurens, H. Parrinello, and
M. Joron. Mutation accumulation in chromosomal inversions maintains wing pat-
726 tern polymorphism in a butterfly. bioRxiv, 2019. 10.1101/736504. URL
<https://www.biorxiv.org/content/early/2019/08/15/736504>.

728 Y. Jiang, D. I. Bolnick, and M. Kirkpatrick. Assortative mating in animals. The American
Naturalist, 181(6):E125–E138, 2013. 10.1086/670160. URL <https://doi.org/10.1086/670160>.
730 PMID: 23669548.

M. Joron and Y. Iwasa. The evolution of a müllerian mimic in a spatially distributed community.
732 Journal of Theoretical Biology, 237(1):87–103, 2005.

M. Joron, I. R. Wynne, G. Lamas, and J. Mallet. Variable selection and the coexistence of multiple
734 mimetic forms of the butterfly heliconius numata. Evolutionary Ecology, 13(7-8):721–754, 1999.

M. Joron, R. Papa, M. Beltrán, N. Chamberlain, J. Mavárez, S. Baxter, M. Abanto, E. Bermingham,
736 S. J. Humphray, J. Rogers, et al. A conserved supergene locus controls colour pattern diversity
in heliconius butterflies. PLoS biology, 4(10):e303, 2006.

738 M. Joron, L. Frezal, R. T. Jones, N. L. Chamberlain, S. F. Lee, C. R. Haag, A. Whibley, M. Be-
cuwe, S. W. Baxter, L. Ferguson, et al. Chromosomal rearrangements maintain a polymorphic
740 supergene controlling butterfly mimicry. Nature, 477(7363):203, 2011.

M. Kirkpatrick. How and why chromosome inversions evolve. PLoS biology, 8(9):e1000501, 2010.

742 M. Kirkpatrick and S. L. Nuismer. Sexual selection can constrain sympatric speciation.
Proceedings of the Royal Society of London. Series B: Biological Sciences, 271(1540):687–693,
744 2004.

- M. Kopp, M. R. Servedio, T. C. Mendelson, R. J. Safran, R. L. Rodríguez, M. E. Hauber, E. C.
746 Scordato, L. B. Symes, C. N. Balakrishnan, D. M. Zonana, et al. Mechanisms of assortative
mating in speciation with gene flow: connecting theory and empirical research. The American
748 Naturalist, 191(1):1–20, 2018.
- M. R. Kronforst, L. G. Young, D. D. Kapan, C. McNeely, R. J. O’Neill, and L. E. Gilbert. Linkage
750 of butterfly mate preference and wing color preference cue at the genomic location of wingless.
Proceedings of the National Academy of Sciences, 103(17):6575–6580, 2006.
- 752 Y. Kuang and Y. Takeuchi. Predator-prey dynamics in models of prey dis-
persal in two-patch environments. Mathematical Biosciences, 120(1):77 – 98,
754 1994. ISSN 0025-5564. [https://doi.org/10.1016/0025-5564\(94\)90038-8](https://doi.org/10.1016/0025-5564(94)90038-8). URL
<http://www.sciencedirect.com/science/article/pii/0025556494900388>.
- 756 C. Küpper, M. Stocks, J. E. Risse, N. dos Remedios, L. L. Farrell, S. B. McRae, T. C. Morgan,
N. Karlionova, P. Pinchuk, Y. I. Verkuil, A. S. Kitaysky, J. C. Wingfield, T. Piersma, K. Zeng,
758 J. Slate, M. Blaxter, D. B. Lank, and T. Burke. A supergene determines highly divergent male
reproductive morphs in the ruff. Nature Genetics, 48(1):79–83, 2016. 10.1038/ng.3443. URL
760 <https://doi.org/10.1038/ng.3443>.
- Y. Le Poul, A. Whibley, M. Chouteau, F. Prunier, V. Llaurens, and M. Joron. Evolution of domi-
762 nance mechanisms at a butterfly mimicry supergene. Nature Communications, 5:5644, 2014.
- V. Llaurens, L. Gonthier, and S. Billiard. The sheltered genetic load linked to the s locus in plants:
764 new insights from theoretical and empirical approaches in sporophytic self-incompatibility.
Genetics, 183(3):1105–1118, 2009.
- 766 V. Llaurens, S. Billiard, and M. Joron. The effect of dominance on polymorphism in müllerian
mimicry. Journal of theoretical biology, 337:101–110, 2013.
- 768 J. Mallet and N. H. Barton. Strong natural selection in a warning-color hybrid zone. Evolution,
43(2):421–431, 1989. ISSN 00143820, 15585646. URL <http://www.jstor.org/stable/2409217>.

770 C. Mérot, V. Llaurens, E. Normandeau, L. Bernatchez, and M. Wellenreuther. Balancing selection
via life-history trade-offs maintains an inversion polymorphism in a seaweed fly. bioRxiv, 2019.
772 10.1101/648584. URL <https://www.biorxiv.org/content/early/2019/05/24/648584>.

R. M. Merrill, P. Rastas, S. H. Martin, M. C. Melo, S. Barker, J. Davey, W. O. McMillan, and C. D.
774 Jiggins. Genetic dissection of assortative mating behavior. PLoS biology, 17(2):e2005902, 2019.

F. Müller. Ituna and thyridia; a remarkable case of mimicry in butterflies (transl. by ralph meldola
776 from the original german article in kosmos, may 1879, 100). Transactions of the Entomological
Society of London, 1879.

778 S. P. Otto, M. R. Servedio, and S. L. Nuismer. Frequency-dependent selection and the evolution
of assortative mating. Genetics, 179(4):2091–2112, 2008.

780 D. J. Penn and W. K. Potts. The evolution of mating preferences and major histocompatibility
complex genes. The American Naturalist, 153(2):145–164, 1999.

782 S. Piertney and M. Oliver. The evolutionary ecology of the major histocompatibility complex.
Heredity, 96(1):7, 2006.

784 T. N. Sherratt. Spatial mosaic formation through frequency-dependent selection in müllerian
mimicry complexes. Journal of Theoretical Biology, 2006.

786 X. Thibert-Plante and S. Gavrillets. Evolution of mate choice and the so-called magic traits in
ecological speciation. Ecology letters, 16, 06 2013. 10.1111/ele.12131.

788 J. W. Thomas, M. Cáceres, J. J. Lowman, C. B. Morehouse, M. E. Short, E. L. Baldwin, D. L. Maney,
and C. L. Martin. The chromosomal polymorphism linked to variation in social behavior in the
790 white-throated sparrow (*zonotrichia albicollis*) is a complex rearrangement and suppressor of
recombination. Genetics, 179(3):1455–1468, 2008. ISSN 0016-6731. 10.1534/genetics.108.088229.
792 URL <https://www.genetics.org/content/179/3/1455>.

- 794 H. B. Thronycroft. A cytogenetic study of the white-throated sparrow, *zonotrichia albicollis* (gmelin). Evolution, 29(4):611–621, 1975. ISSN 00143820, 15585646. URL <http://www.jstor.org/stable/2407072>.
- 796 T. Tregenza and N. Wedell. Genetic compatibility, mate choice and patterns of parentage: invited review. Molecular Ecology, 9(8):1013–1027, 2000.
- 798 E. M. Tuttle, A. O. Bergland, M. L. Korody, M. S. Brewer, D. J. Newhouse, P. Minx, M. Stager, A. Betuel, Z. A. Cheviron, W. C. Warren, et al. Divergence and functional degradation of a sex
800 chromosome-like supergene. Current Biology, 26(3):344–350, 2016.
- J. Wang, Y. Wurm, M. Nipitwattanaphon, O. Riba-Grognuz, Y.-C. Huang, D. Shoemaker, and L. Keller. A y-like social chromosome causes alternative colony organization in fire ants. Nature, 493(7434):664–668, 2013. 10.1038/nature11832. URL
802 <https://doi.org/10.1038/nature11832>.
- 804 C. Wedekind and S. Furi. Body odour preferences in men and women: do they aim for specific
806 mhc combinations or simply heterozygosity? Proceedings of the Royal Society of London. Series B: Biological Sciences, 264(1387):1471–1479, 1997.
- 808 C. Wedekind, T. Seebeck, F. Bettens, and A. J. Paepke. Mhc-dependent mate preferences in
humans. Proceedings of the Royal Society of London. Series B: Biological Sciences, 260(1359):
810 245–249, 1995.
- E. L. Westerman, N. W. VanKuren, D. Massardo, A. Tenger-Trolander, W. Zhang, R. I. Hill,
812 M. Perry, E. Bayala, K. Barr, N. Chamberlain, et al. Aristaless controls butterfly wing color
variation used in mimicry and mate choice. Current Biology, 28(21):3469–3474, 2018.
- 814 S. Wright. The distribution of self-sterility alleles in populations. Genetics, 24(4):538, 1939.

S1: Mendelian segregation

816 To compute the proportion of a given genotype in the progeny of the different crosses occurring
in the population, we define a function $coef(g^O, g^M, g^F, \rho)$ summarizing the Mendelian segrega-
818 tion of alleles assuming two diploid loci and a rate of recombination ρ between these loci. Let
 $g^O = (p_m^O, p_f^O, m_m^O, m_f^O)$, $g^M = (p_m^M, p_f^M, m_m^M, m_f^M)$ and $g^F = (p_m^F, p_f^F, m_m^F, m_f^F)$ be the offspring, ma-
820 ternal and paternal genotypes respectively, all in \mathcal{G} . For $I \in \{O, M, F\}$, p_m^I and m_m^I (resp. p_f^I
and m_f^I) are the alleles on the maternal (resp. paternal) chromosomes. $coef(g^O, g^M, g^F, \rho)$ is the
822 average proportion of genotype g^O in the progeny of a mother of genotype g^M mating with a
father of genotype g^F given a recombination rate ρ .

824 Each diploid mother can produce four types of haploid gametes containing alleles (p_m^M, m_m^M) ,
 (p_f^M, m_f^M) , (p_f^M, m_m^M) or (p_m^M, m_f^M) , in proportion $\frac{1-\rho}{2}, \frac{1-\rho}{2}, \frac{\rho}{2}$ and $\frac{\rho}{2}$ respectively. Then the propor-
826 tion of gametes with alleles $(p, m) \in \mathcal{A}_P \times \mathcal{A}_M$ produced by the mother is given by the function
 $coef_{haplotype}(p, m, g^M, \rho)$, where

$$\begin{aligned} coef_{haplotype}(p, m, g^M, \rho) &= \frac{1-\rho}{2} \mathbb{1}_{\{p=p_m^M\}} \mathbb{1}_{\{m=m_m^M\}} + \frac{1-\rho}{2} \mathbb{1}_{\{p=p_f^M\}} \mathbb{1}_{\{m=m_f^M\}} \\ &\quad + \frac{\rho}{2} \frac{1-\rho}{2} \mathbb{1}_{\{p=p_f^M\}} \mathbb{1}_{\{m=m_m^M\}} + \frac{\rho}{2} \frac{1-\rho}{2} \mathbb{1}_{\{p=p_m^M\}} \mathbb{1}_{\{m=m_f^M\}}. \end{aligned}$$

828 Similarly, each diploid father can produce four types of haploid gametes. The propor-
tion of genotype $(p, m) \in \mathcal{A}_P \times \mathcal{A}_M$ in the gametes of a given father is given by the function
830 $coef_{haplotype}(p, m, g^F, \rho)$.

The average proportion of genotype g^O in the progeny of a cross between a mother of geno-
832 type g^M and a father of genotype g^F given a recombination rate ρ is given by:

$$coef(g^O, g^M, g^F, \rho) = coef_{haplotype}(p_m^O, m_m^O, g^M, \rho) coef_{haplotype}(p_f^O, m_f^O, g^F, \rho).$$

S2: Checking of the computed genotype frequencies in the progeny of all crosses

834

We then check that the sum of the computed frequencies of the different genotypes i in the
836 progeny of all crosses occurring in patch n ($(F_{i,n})_{i \in \mathcal{G}}$ for $n \in \{1, 2\}$) actually equals to one. Let n
be in $\{1, 2\}$, we have:

$$\begin{aligned}
 \sum_{i \in \mathcal{G}} F_{i,n} &= \sum_{i \in \mathcal{G}} \sum_{(j,k) \in \mathcal{G}^2} \text{coef}(i, j, k, \rho) f_{j,n} \frac{M_{j,n}}{\overline{M}_n} \text{Pref}_{j,CP(k)} \frac{f_{k,n}}{T_{j,n}}, \\
 &= \sum_{(j,k) \in \mathcal{G}^2} f_{j,n} \frac{M_{j,n}}{\overline{M}_n} \text{Pref}_{j,CP(k)} \frac{f_{k,n}}{T_{j,n}} \underbrace{\sum_{i \in \mathcal{G}} \text{coef}(i, j, k, \rho)}_{=1}, \\
 &= \sum_{j \in \mathcal{G}} f_{j,n} \frac{M_{j,n}}{\overline{M}_n} \frac{\sum_{k \in \mathcal{G}} \text{Pref}_{j,CP(k)} f_{k,n}}{T_{j,n}}, \\
 &= \sum_{j \in \mathcal{G}} f_{j,n} \frac{M_{j,n}}{\overline{M}_n} \frac{\sum_{k \in \mathcal{G}} (\mathbb{1}_{\{CP(k)=A\}} + \mathbb{1}_{\{CP(k)=B\}} + \mathbb{1}_{\{CP(k)=C\}}) \text{Pref}_{j,CP(k)} f_{k,n}}{T_{j,n}}
 \end{aligned}$$

because $\forall k \in \mathcal{G}, \quad \mathbb{1}_{\{CP(k)=A\}} + \mathbb{1}_{\{CP(k)=B\}} + \mathbb{1}_{\{CP(k)=C\}} = 1,$

$$\begin{aligned}
 &= \sum_{j \in \mathcal{G}} f_{j,n} \frac{M_{j,n}}{\overline{M}_n} \frac{\sum_{k \in \mathcal{G}} \mathbb{1}_{\{CP(k)=A\}} \text{Pref}_{j,A} f_{k,n} + \sum_{k \in \mathcal{G}} \mathbb{1}_{\{CP(k)=B\}} \text{Pref}_{j,B} f_{k,n} + \sum_{k \in \mathcal{G}} \mathbb{1}_{\{CP(k)=C\}} \text{Pref}_{j,C} f_{k,n}}{T_{j,n}}, \\
 &= \sum_{j \in \mathcal{G}} f_{j,n} \frac{M_{j,n}}{\overline{M}_n} \frac{\text{Pref}_{j,A} \sum_{k \in \mathcal{G}} \mathbb{1}_{\{CP(k)=A\}} f_{k,n} + \text{Pref}_{j,B} \sum_{k \in \mathcal{G}} \mathbb{1}_{\{CP(k)=B\}} f_{k,n} + \text{Pref}_{j,C} \sum_{k \in \mathcal{G}} \mathbb{1}_{\{CP(k)=C\}} f_{k,n}}{T_{j,n}}, \\
 &= \sum_{j \in \mathcal{G}} f_{j,n} \frac{M_{j,n}}{\overline{M}_n} \frac{\text{Pref}_{j,A} P_{A,n} + \text{Pref}_{j,B} P_{B,n} + \text{Pref}_{j,C} P_{C,n}}{T_{j,n}}, \\
 &= \sum_{j \in \mathcal{G}} f_{j,n} \frac{M_{j,n}}{\overline{M}_n} \frac{T_{j,n}}{T_{j,n}}, \\
 &= \sum_{j \in \mathcal{G}} f_{j,n} \frac{M_{j,n}}{\overline{M}_n}, \\
 &= \frac{\overline{M}_n}{\overline{M}_n}, \\
 &= 1.
 \end{aligned}$$

S3: Numerical resolution

In this study, we used a numerical scheme to simulate our dynamical system. For $(i, n) \in \mathcal{G} \times \{1, 2\}$, let $N_{i,n}^t$ be the numerical approximation of $N_{i,n}(t)$. We use an explicit Euler scheme, therefore we approximate the quantity $\frac{d}{dt}N_{i,n}(t)$ by

$$\frac{N_{i,n}^{t+\Delta t} - N_{i,n}^t}{\Delta t},$$

with Δt being the step time in our simulations.

For $(i, n) \in \mathcal{G} \times \{1, 2\}$, an approximation of equation 1 becomes:

$$\frac{N_{i,n}^{t+\Delta t} - N_{i,n}^t}{\Delta t} = \text{Pred}_{i,n}^t + \text{Mort}_{i,n}^t + \text{Mig}_{i,n}^t + \text{Rep}_{i,n}^t.$$

This equation is equivalent to:

$$N_{i,n}^{t+\Delta t} = N_{i,n}^t + \Delta t \left(\text{Pred}_{i,n}^t + \text{Mort}_{i,n}^t + \text{Mig}_{i,n}^t + \text{Rep}_{i,n}^t \right).$$

Given $(N_{i,n}^0)_{(i,n) \in \mathcal{G} \times \{1,2\}}$, we can simulate an approximation of the dynamical system.

S4: Numerical approximation of equilibrium states

To estimate the equilibrium reached by our dynamical system using simulations assuming different initial conditions, we define the variable Var^t quantifying the change in the numerical solution :

$$Var^t = \sqrt{\sum_{(i,n) \in \mathcal{G} \in \{1,2\}} \left(\frac{N_{i,n}^{t+\Delta t} - N_{i,n}^t}{\Delta t} \right)^2}.$$

When $\frac{Var^t}{N_{tot}} < 10^{-5}$, we assume that the dynamical system has reached equilibrium, with N_{tot} being the total density in both patches.

Supplementary Figures

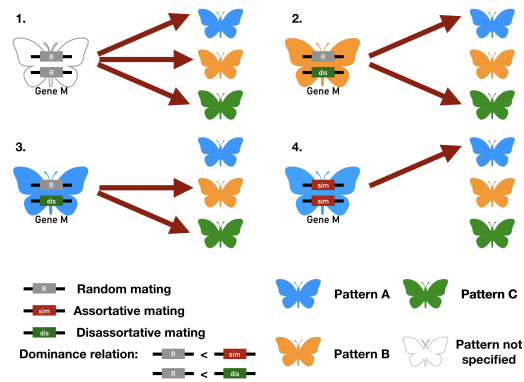


Figure S5: Mate preferences expressed by individuals carrying different genotypes at the preference locus *M*, assuming *self-referencing* (hyp. 1). 1. Butterflies carrying two *r* alleles mate at random, independently of either their own color pattern or the color pattern displayed by mating partners. 2-3. Butterflies carrying a *dis* allele display disassortative mating, and mate preferentially with individuals with a color pattern different from their own. 4. Butterflies carrying a *sim* allele display an assortative mating behavior and therefore preferentially mate with individuals displaying the same color pattern. Cases 1 and 4 therefore lead to *self-acceptance*, while cases 2 and 3 lead to *self-avoidance*.

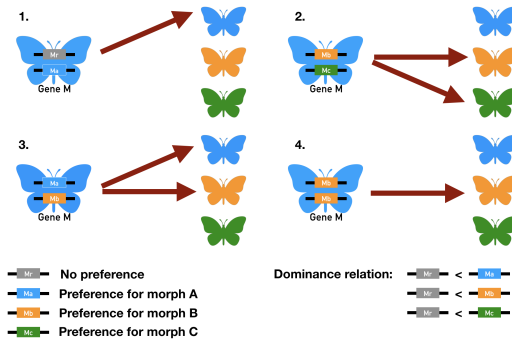


Figure S6: Mate preferences expressed by individuals carrying different genotypes at the preference locus *M*, assuming preference alleles encoding for attraction of specific color patterns (*recognition/trait*) (hyp. 2.a). 1. A butterfly displaying phenotype *A* (in blue) carries one allele coding for specific attraction toward partners displaying phenotype *A* (in blue) and the allele coding for random mating at the locus *M* controlling the mate choice. This butterfly will mate preferentially with individuals displaying phenotype *A*, resulting in assortative mating. 2. A butterfly displaying phenotype *A* (in blue) carries one allele coding for specific attraction toward partner displaying phenotype *B* (in orange) and one allele coding for specific attraction toward partners displaying phenotype *C* (in green). This individual will preferentially mate with individuals displaying phenotype *B* and *C*, resulting in disassortative mating. 3. A butterfly displaying phenotype *A* (in blue) carries one allele coding for specific attraction toward partner displaying phenotype *A* (in blue) and one allele coding for specific attraction toward partners displaying phenotype *B* (in orange). This individual will preferentially mate with individuals displaying phenotype *A* and *B*. 4. A butterfly displaying phenotype *A* (in blue) carries two alleles coding for specific attraction toward partner displaying phenotype *B* (in orange). This individual will preferentially mate with individuals displaying phenotype *B*, resulting in disassortative mating. Cases 1 and 3 therefore lead to *self-acceptance*, while cases 2 and 4 lead to *self-avoidance*.

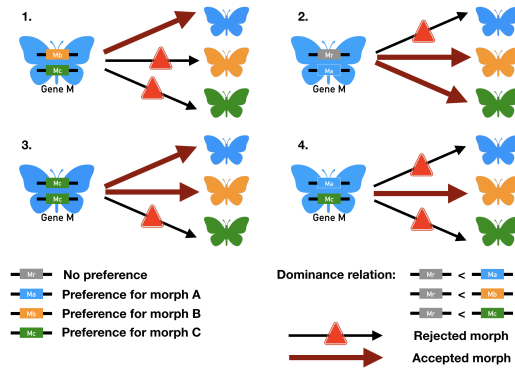


Figure S7: Mate preferences expressed by the different individuals carrying different genotypes at the preference locus *M*, assuming preference alleles encoding for rejection of specific color patterns (*recognition/trait*) (hyp. 2.a). 1. A butterfly displaying phenotype *A* (in blue) carries one allele coding for specific rejection toward partners displaying phenotype *B* (in orange) and one allele coding for specific rejection toward partners displaying phenotype *C* (in orange). This butterfly will mate preferentially with individuals displaying phenotype *A*, resulting in assortative mating. 2. A butterfly displaying phenotype *A* (in blue) carries one allele coding for specific rejection toward partners displaying phenotype *A* (in orange) and one allele coding for random mating (in grey). This butterfly will mate preferentially with individuals displaying phenotypes *B* and *C*, resulting in disassortative mating. 3. A butterfly displaying phenotype *A* (in blue) carries two alleles coding for specific rejection toward partners displaying phenotype *C* (in green). This butterfly will mate preferentially with individuals displaying phenotypes *A* and *B*. 4. A butterfly displaying phenotype *A* (in blue) carries one allele coding for specific rejection toward partners displaying phenotype *A* (in blue) and one allele coding for specific rejection toward partners displaying phenotype *C* (in green). This butterfly will mate preferentially with individuals displaying phenotype *B* resulting in disassortative mating. Cases 1 and 3 therefore lead to *self-acceptance*, while cases 2 and 4 lead to *self-avoidance*.

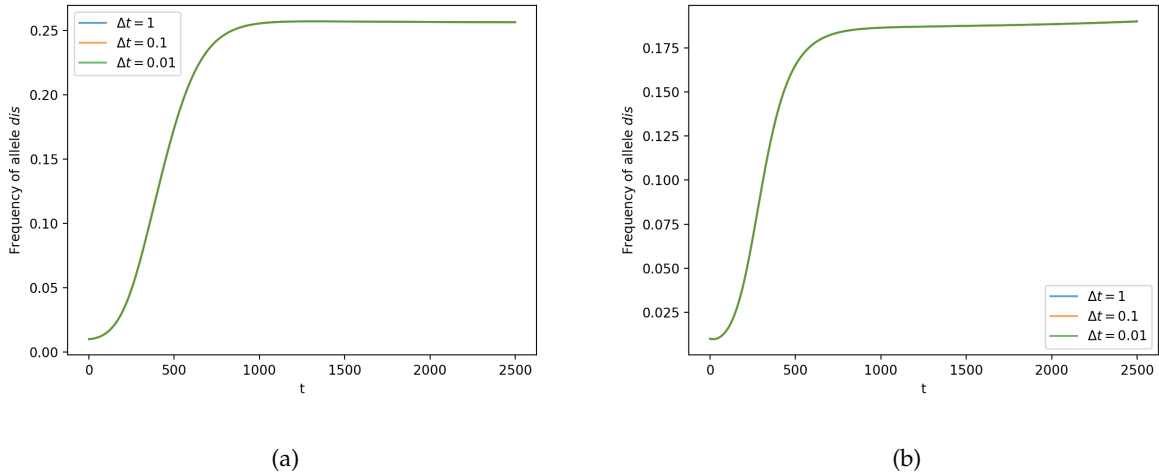
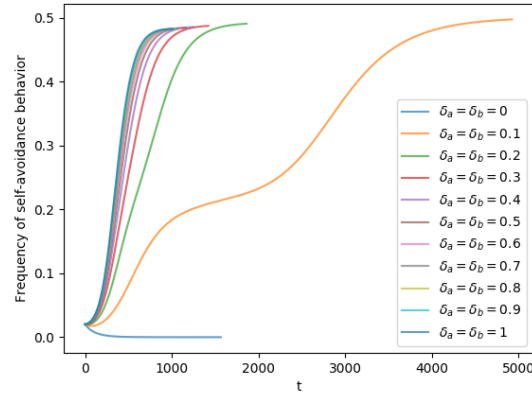


Figure S8: Evolution of the proportion of a mutant *dis* in the population immediately after its introduction, using simulations with three different time units ($\Delta t = 1$ in blue, $\Delta t = 0.1$ in orange or $\Delta t = 0.01$ in green), under the *self-referencing hypothesis* (hyp. 1). All simulations give similar dynamics, assuming (a) $\delta_a = \delta_b = 0.5$, $\delta_c = 0$ or (b) $\delta_a = \delta_b = \delta_c = 0.2$, confirming that using discrete time simulations provides relevant estimations of the evolution of disassortative mating. Simulations are run during 2500 time steps and assuming $r = 1$, $K = 2000$, $N_{tot,1}^0 = N_{tot,2}^0 = 100$, $\lambda = 0.0002$, $d_m = 0.05$, $d_{n-m} = 0.15$, $\rho = 0$, $mig = 0.1$, $\delta = 0.1$ and $c_r = 0.1$.

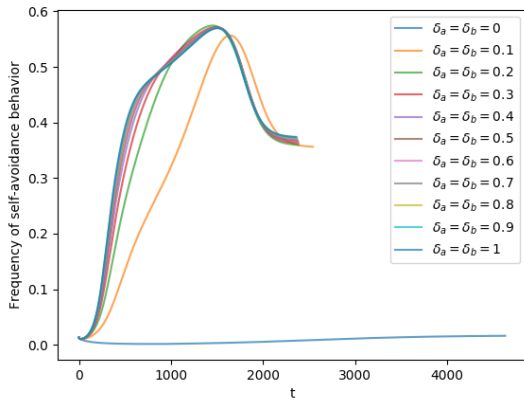
$\delta_1 = \delta_2$	δ_3	Population 1			Population 2		
		Proportion of morph A	Proportion of morph B	Proportion of morph C	Proportion of morph A	Proportion of morph B	Proportion of morph C
0,00	0,00	90,5 %	9,5 %	0,0 %	49,8 %	50,2 %	0,0 %
0,00	0,25	90,5 %	9,5 %	0,0 %	49,8 %	50,2 %	0,0 %
0,00	0,50	90,5 %	9,5 %	0,0 %	49,8 %	50,2 %	0,0 %
0,00	1,00	90,5 %	9,5 %	0,0 %	49,8 %	50,2 %	0,0 %
0,25	0,00	61,8 %	7,7 %	30,6 %	22,3 %	52,1 %	25,6 %
0,25	0,25	78,8 %	17,9 %	3,3 %	36,2 %	57,6 %	6,2 %
0,25	0,50	80,5 %	17,8 %	1,7 %	39,3 %	57,2 %	3,5 %
0,25	1,00	81,6 %	17,6 %	0,8 %	41,5 %	56,6 %	1,8 %
0,50	0,00	54,5 %	5,7 %	39,8 %	18,7 %	49,6 %	31,7 %
0,50	0,25	76,3 %	18,6 %	5,1 %	33,9 %	57,8 %	8,3 %
0,50	0,50	78,7 %	18,7 %	2,6 %	37,5 %	57,7 %	4,8 %
0,50	1,00	80,2 %	18,5 %	1,3 %	40,2 %	57,3 %	2,5 %
1,00	0,00	49,9 %	4,6 %	45,5 %	16,9 %	47,7 %	35,4 %
1,00	0,25	74,6 %	18,9 %	6,5 %	32,7 %	57,4 %	9,8 %
1,00	0,50	77,5 %	19,1 %	3,3 %	36,6 %	57,7 %	5,7 %
1,00	1,00	79,3 %	19,0 %	1,7 %	39,6 %	57,4 %	3,0 %

Figure S9: **Influence of genetic load on color pattern polymorphism, assuming random mating.**

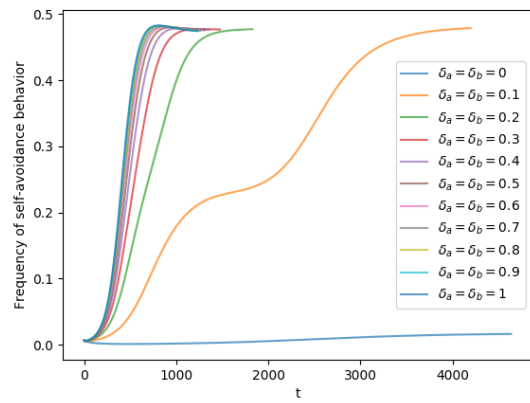
The proportions of phenotypes *A*, *B* and *C* in the populations living in patch 1 and 2 respectively at equilibrium depend on the different values of genetic load associated with the dominant allele *a* (δ_a), intermediate-dominant allele *b* (δ_b) and recessive allele *c* (δ_c). Simulations are run assuming $r = 1$, $K = 2000$, $N_{tot,1}^0 = N_{tot,2}^0 = 100$, $\lambda = 0.0002$, $d_m = 0.05$, $d_{n-m} = 0.15$, $\rho = 0$, $mig = 0.1$, $\delta = 0.1$ and $c_r = 0.1$.



(a)



(b)



(c)

Figure S10: **Frequency of self-avoidance behavior at the population level through time for different levels of genetic load, assuming (a) self-referencing (hyp. 1), (b) attraction rule (hyp. 2.a) or (c) rejection rule (hyp. 2.b) at the preference locus (recognition/trait).** The evolution of the proportion of individuals displaying self-avoidance P_{s-av} after the introduction of preference alleles until equilibrium are shown for different values of genetic load δ_a and δ_b . Simulations are run assuming $r = 1$, $K = 2000$, $N_{tot,1}^0 = N_{tot,2}^0 = 100$, $\lambda = 0.0002$, $d_m = 0.05$, $d_{n-m} = 0.15$, $\rho = 0$, $mig = 0.1$, $\delta_c = 0$, $\delta = 0.1$ and $c_r = 0.1$.

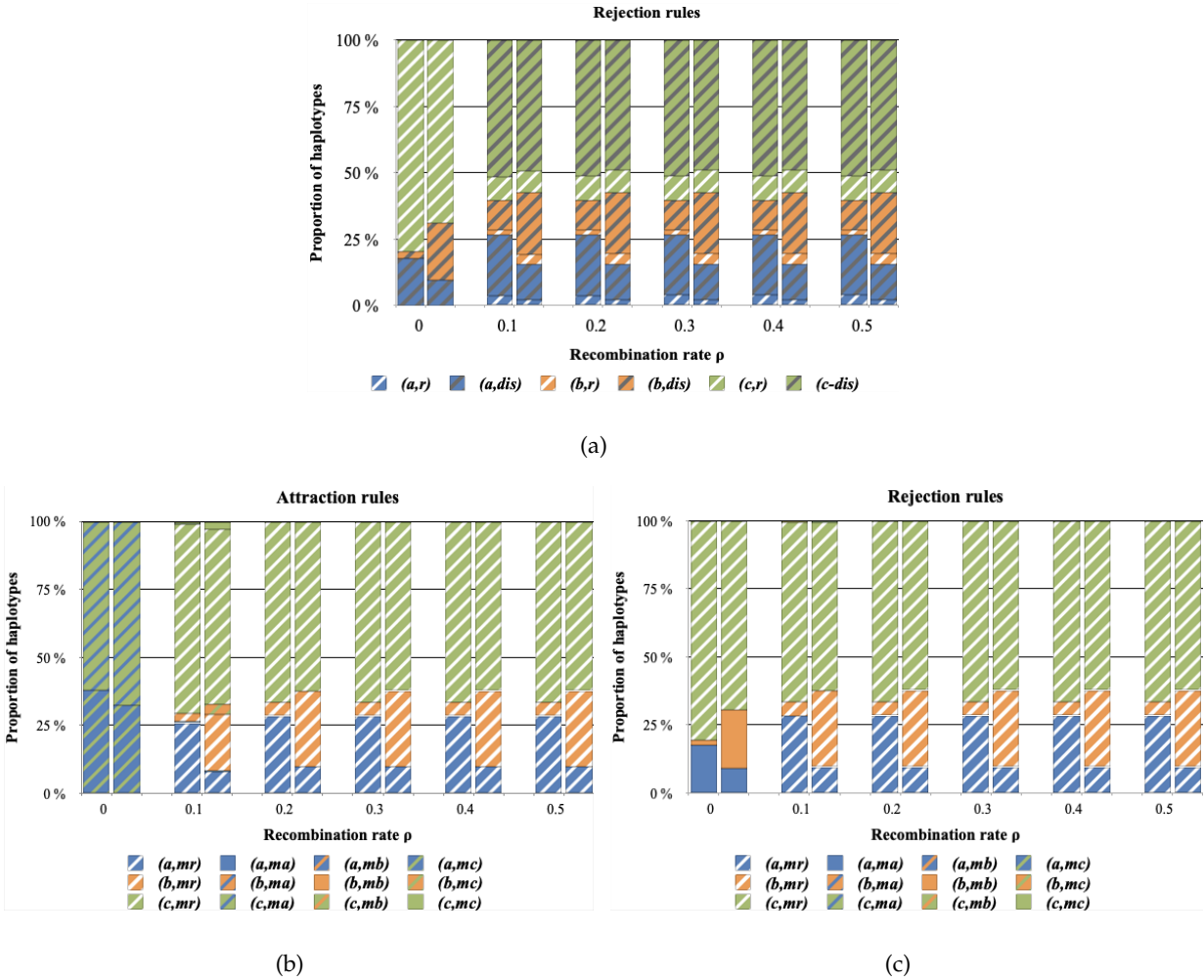


Figure S11: Influence of the recombination between color pattern and preference alleles on haplotype diversity, assuming (a) *self-referencing* (hyp. 1), (b) *attraction rule* (hyp. 2.a) or (c) *rejection rule* (hyp. 2.b) at the preference locus (*recognition/trait*). The proportion of haplotypes at equilibrium after the introduction of preference alleles in both patches are shown for different values of recombination rate ρ between the preference locus M and the color pattern locus P . For each value of recombination rate (ρ) the first and second bars represented haplotype proportions in the populations living in the patch 1 and 2 respectively. Simulations are run assuming $r = 1$, $K = 2000$, $N_{tot,1}^0 = N_{tot,2}^0 = 100$, $\lambda = 0.0002$, $d_m = 0.05$, $d_{n-m} = 0.15$, $mig = 0.1$, $\delta_a = \delta_b = 0.5$, $\delta_c = 0$, $\delta = 0.1$ and $c_r = 0.1$.